Inorganic Chemistry

Article

pubs.acs.org/IC

pH-Specific Hydrothermal Assembly of Binary and Ternary Pb(II)-(O,N-Carboxylic Acid) Metal Organic Framework Compounds: Correlation of Aqueous Solution Speciation with Variable Dimensionality Solid-State Lattice Architecture and Spectroscopic Signatures

C. Gabriel,[†] M. Perikli,[†] C. P. Raptopoulou,[‡] A. Terzis,[‡] V. Psycharis,[‡] C. Mateescu,[§] T. Jakusch,[∥] T. Kiss,[∥] M. Bertmer,[⊥] and A. Salifoglou*[,†]

[†]Department of Chemical Engineering, Laboratory of Inorganic Chemistry, Aristotle University of Thessaloniki, Thessaloniki 54124, Greece

[‡]Institute of Materials Science, NCSR "Demokritos", Aghia Paraskevi 15310, Attiki, Greece

[§]Banat's University of Agricultural Sciences and Veterinary Medicine, Timisoara 300645, Romania

[∥]Biocoordination Chemistry Research Group of the Hungarian Academy of Sciences, Department of Inorganic and Analytical Chemistry, University of Szeged, Szeged H-6720, Hungary

[⊥]Institut für Experimentelle Physik II, Universität Leipzig, Leipzig 04103, Germany

Supporting Information

ABSTRACT: Hydrothermal pH-specific reactivity in the binary/ternary systems of Pb(II) with the carboxylic acids *N*-hydroxyethyliminodiacetic acid (Heida), 1,3-diamino-2-hydroxypropane-*N*,*N*,*N*′,*N*′-tetraacetic acid (Dpot), and 1,10-phenanthroline (Phen) afforded the new well-defined crystalline compounds $[Pb(Heida)]_n \cdot nH_2O$(**1**), $[Pb(Phen)(Heida)] \cdot 4H_2O$(**2**), and $[Pb_3(NO_3)(Dpot)]_n$(**3**). All compounds were characterized by elemental analysis, FT-IR, solution or/and solid-state NMR, and single-crystal X-ray diffraction. The structures in **1**−**2** reveal the presence of a Pb(II) center coordinated to one Heida ligand, with **1** exhibiting a two-dimensional (2D) lattice extending to a three-dimensional (3D) one through H-bonding interactions. The concurrent aqueous speciation study of the binary Pb(II)−Heida system projects species complementing the synthetic efforts, thereby lending credence to a global structural speciation strategy in investigating binary/ternary Pb(II)-Heida/Phen systems. The involvement of Phen in **2** projects the significance of nature and reactivity potential of N-aromatic chelators, disrupting the binary lattice in **1** and influencing the nature of the ultimately arising ternary 3D lattice. **3** is a ternary coordination polymer, where Pb(II)-Dpot coordination leads to a 2D metal−organic-framework material with unique architecture. The collective physicochemical properties of **1**−**3** formulate the salient features of variable dimensionality metal−organic-framework lattices in binary/ternary Pb(II)-(hydroxycarboxylate) structures, based on which new Pb(II) materials with distinct architecture and spectroscopic signature can be rationally designed and pursued synthetically.

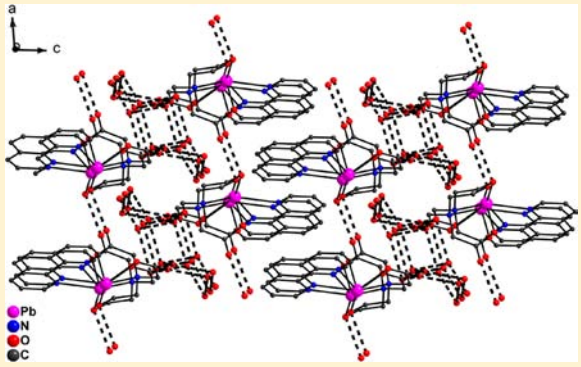

INTRODUCTION

The synthesis of discrete and polymeric metal−organic complexes is currently attracting considerable attention because of their unique structural topologies and properties. Building new complexes and modifying their architectures to study their physical properties has been a topic for many research groups.[1] Lead, a heavy toxic metal, is commonly encountered in critical life cycles because of its widespread use in numerous industrial applications and its occurrence in the environment.[2] The diversity of lead use entails an equally diverse chemical reactivity toward organic and inorganic substrates, ultimately leading to numerous products. The incumbent chemical reactivity is intimately associated with the nature and properties of Pb(II) and the reacting partners in the involved reaction mixtures. To this end, good knowledge of the coordination chemistry leading to preferential binding of lead over other (non)essential metal ions is crucial for understanding the toxicological properties of Pb(II), the design of selective chelation therapy agents, and the development of efficient chelating agents for the remediation of polluted water and soil. The most common chelator studied in the literature is EDTA, which has been used to remove lead

Received: April 25, 2012
Published: August 17, 2012

nitrate from wastewater. A congener ligand, Dpot, (1,3-diamino-2-hydroxypropane-*N*,*N*,*N*′,*N*′-tetraacetic acid) is an analogue of ethylenediamine-*N*,*N*,*N*′,*N*′-tetraacetic acid (EDTA). The chemical reactivity of Dpot involves employment of all four carboxylic acid terminals and is further exemplified by the presence of the central alcohol function, useful in promoting dinuclear metal unit formation as an alkoxide bridge between two metal ions.[3−5]

Analogous to Dpot ligand is Heida, which is simpler than Dpot and also possesses the same coordination groups. Both Dpot and Heida ligands can lead to the formation of monomers, dimers, or polymers. Coordination polymers constitute one of the most important classes of organic−inorganic hybrid materials, which have attracted great research interest not only because of their intriguing variety of architectures and topologies but also because of their fascinating potential applications in functional solid materials, ion exchange, catalysis, and the development of optical, electronic, and magnetic devices.[6−8]

Consequently, a variety of coordination polymers of variable M(II)-L composition have been constructed by careful selection of the metal ions and multidentate bridging ligands L. Dpot and Heida are two very promising multidentate bridging ligands. Encouraged by successful efforts in our lab to employ hydrothermal synthesis for the assembly of crystalline materials containing Pb(II), we used this method for the synthesis, isolation, and crystallization of new binary and ternary compounds of Pb(II) with variable nature O,N-containing aromatic and carboxylic acid ligands. In an effort to delve into the molecular factors dictating the assembly of binary and ternary Pb(II)-alcohol-containing carboxylic acid materials, a global structural speciation approach was adopted for the synthesis and solution investigation of binary and ternary systems involving Heida and Dpot ligands. To this end, we report herein on (a) the aqueous speciation studies of the binary Pb(II)-Heida system, and (b) the hydrothermal synthesis of binary and ternary Pb(II)-Heida/Phenanthroline and Pb(II)-Dpot materials, where in a unique way formation of three new compounds is achieved, containing Pb(II)-Heida, Pb(II)-Heida-Phenanthroline, and Pb(II)-Dpot. Physicochemical characterization of all emerging synthetic species (a) projects the characteristic features emerging from both solution and structural studies, emphasizing the association of the spectroscopic signature with the assembly of variable dimensionality lattice architectures encountered in **1**−**3**, and (b) suggests potential pathways furthering use of **1**−**3** as precursors to hydrothermally synthesized new materials with distinctly differentiated structural and spectroscopic signature(s).

EXPERIMENTAL SECTION

Materials and Methods. All experiments were carried out in air. Nanopure quality water was used for all reactions. $Pb(NO_3)_2$, $Pb(CH_3COO)_2{\cdot}3H_2O$, *N*-hydroxyethyl-iminodiacetic acid (Heida), 1,3-diamino-2-hydroxypropane-*N*,*N*,*N*′,*N*′-tetraacetic acid (Dpot), and sodium hydroxide were purchased from Fluka. 1,10-Phenanthroline (Phen) was supplied by Aldrich.

Physical Measurements. FT-Infrared spectra were recorded on a Thermo, Nicolet IR 200 FT-infrared spectrometer. A ThermoFinnigan Flash EA 1112 CHNS elemental analyzer was used for the simultaneous determination of carbon, hydrogen, and nitrogen (%). The analyzer operation is based on the dynamic flash combustion of the sample (at 1800 °C) followed by reduction, trapping, complete GC separation, and detection of the products. The instrument is (a) fully automated and is controlled by a PC via the Eager 300 dedicated software, and (b) capable of handling solid, liquid, or gaseous substances.

Solution NMR Spectroscopy. Solution ^{13}C NMR experiments for **1** were carried out on a Varian 600 MHz spectrometer. The sample concentration was approximately 0.02−0.10 M. The compound was dissolved in D_2O. The ^{13}C spectral width was 30000 Hz. Experimental data were processed using VNMR routines. Spectra were zero-filled twice and apodized with a squared sine bell function shifted by $\pi/2$ in both dimensions. Chemical shifts (δ) are reported in parts per million (ppm) relative to the TMS resonance peak.

Solid State NMR Spectroscopy. The solid state ^{13}C CP-MAS NMR spectrum of **1** was obtained on a Bruker Avance 400 NMR spectrometer at a frequency of 100.61 MHz. The spinning rate used was 10.0 kHz at room temperature. The solid-state spectrum of **1** was a result of the accumulation of 1187 scans. The recycle delay used was 10 s, the ^1H 90° pulse length 3 μs, and the contact time 2 ms. All solid-state spectra were externally referenced to TMS with adamantane as a secondary reference.

Solid state CP-MAS ^{13}C NMR spectra for **2** and **3** were obtained on a Varian 400 MHz spectrometer operating at 100.53 MHz. In each case, sufficient sample quantity was placed in a 3.2 mm rotor. A double resonance HX probe was used. The spinning rate was set at 12 kHz. The RAMP-CP pulse sequence of the VnmrJ library was applied, whereby the ^{13}C spin-lock amplitude is varied linearly during CP, while the ^1H spin-lock amplitude is kept constant. RAMP-CP eliminates the Hartmann−Hahn matching profile dependence from the MAS spinning rate and optimizes signal intensity.[9] The solid-state spectra of **2** and **3** were recorded with 5000 scans, using a 90° pulse width of 6.0 μs for **2** and 5.4 μs for **3**, a contact pulse of 3.8 ms, and a recycle delay of 10 s for **2** and **3**. Referencing was again done with respect to TMS via adamantane as a secondary reference.

The high resolution solid state natural abundance ^{207}Pb Magic Angle Spinning (MAS) NMR spectra were recorded on a Bruker Avance MSL400 NMR spectrometer at 83.67 MHz, with ^1H high power decoupling. The spinning rate was 7.3 kHz and the measurements were carried out at room temperature. The ^1H 90° pulse was 3 μs and the contact time 2 ms for both **1** and **2**. For **1**, 884 scans with a recycle delay of 100 s, and for **2**, 4229 scans with a recycle delay of 5 s were recorded. The spectra were referenced to $Pb(NO_3)_2$, which showed a resonance at −3473.5 ppm.[10] Analysis of the chemical shift anisotropy was done with the program dmfit.[11] Values of the anisotropy $\Delta\sigma$ and the asymmetry parameter η are provided according to the Haeberlen convention and are the best fits to the individual spinning sideband intensities.[12]

pH-Potentiometric Measurements. The stability constants of the proton and Pb(II) complexes of the title ligand were determined by pH-potentiometric titrations of 25 mL samples in the pH range 2.3−11 or until precipitation occurred, under a purified argon atmosphere. Care was taken to ensure that titrimetric data were recorded and collected under conditions taking into consideration the kinetically sluggish Pb(II). Duplicate titrations were performed. The reproducibility of the titrations was within 0.005 pH units. Titration points obtained when 5 min was not enough to attain pH equilibrium were omitted from the evaluation. The ionic strength was adjusted to 0.20 M with KNO_3. During the measurements, the temperature was maintained at 25 ± 0.1 °C. The titrations were performed with a carbonate-free KOH solution of known concentration (ca. 0.2 M). The ligand concentration was 1.7 mM and the metal/ligand ratios were 1:2, 2:2, 2:4, 4:4, and 1:4. All other experimental conditions were the same as in earlier studies.[13−15]

The pH was measured with a computer-controlled Molspin titration system elaborated for titrations at low concentrations and a Metrohm 6.0234.100 combined glass electrode, calibrated for hydrogen ion concentration according to Irving et al.[16] The concentration stability constants $\beta_{pqr} = [M_pA_qH_r]/[M]^p[A]^q[H]^r$ were calculated with the PSEQUAD computer program.[17,18] The uncertainties (3SD values) of the stability constants are given in parentheses in Table 3.

Preparation of $[Pb(Heida)]_n{\cdot}nH_2O$ (1). A quantity of $Pb(CH_3COO)_2{\cdot}3H_2O$ (0.37 g, 1.0 mmol) was placed in a 25 mL round-bottom flask and dissolved in 10 mL of H_2O. Subsequently, Heida (0.35 g, 2.0 mmol) was added slowly and under continuous stirring. Finally, an aqueous solution of sodium hydroxide was added to adjust the pH to a final value of ∼5. The resulting reaction mixture was allowed to stir for 1/2 h and then was placed in a 23 mL Teflon-lined stainless steel reactor and heated to 160 °C for 85 h. Subsequently, the reactor was allowed to

dx.doi.org/10.1021/ic300850g | Inorg. Chem. 2012, 51, 9282−9296

cool to room temperature. The resulting solution was allowed to stand at room temperature until colorless crystals appeared at the bottom of the vessel. The resulting crystalline material (0.10 g, 48%) was collected by filtration, washed with water, and air-dried. Anal. Calcd for **1**, $[Pb(Heida)]\cdot H_2O$, ($C_6H_{11}O_6NPb$), M_r 390): Calculated: (%) C 18.46, H 2.8, N, 3.6. Found: C 18.55, H 2.7, N 3.5.

Preparation of [Pb(phen)(Heida)]·4H$_2$O (2). A quantity of $Pb(CH_3COO)_2\cdot 3H_2O$ (0.37 g, 1.0 mmol) was placed in a 25 mL round-bottom flask and dissolved in 10 mL of H_2O. Subsequently, Heida (0.35 g, 2.0 mmol) was added slowly and under continuous stirring. Then, phen (0.20 g, 1.0 mmol) was added under stirring. Finally, a solution of sodium hydroxide was employed to adjust the solution pH to a final value of ∼8. The resulting reaction mixture was allowed to stir for 1/2 h. Then, it was placed in a 23 mL Teflon-lined stainless steel reactor and heated to 160 °C for 85 h. Subsequently, the reactor was allowed to cool to room temperature. The emerging solution was allowed to stand at room temperature and after a day colorless crystals appeared at the bottom of the vessel. The resulting crystalline material (0.26 g, 41%) was collected by filtration, washed with water and air-dried. Anal. Calcd for **2**, $[Pb(C_{12}H_8N_2)(C_6H_9O_5N)]\cdot 4H_2O$ (**2**) ($C_{18}H_{25}O_9N_3Pb$, M_r 634.61): Calculated: (%) C 34.1, H 3.9, N 6.6. Found: C 34.3, H 3.7, N 6.2.

Preparation of [Pb$_3$(NO$_3$)(Dpot)]$_n$ (3). A quantity of $Pb(NO_3)_2$ (0.33 g, 1.0 mmol)) was placed in a 25 mL round-bottom flask and dissolved in 10 mL of H_2O. Subsequently, Dpot (0.32 g, 2.0 mmol) was added slowly and under continuous stirring. The final pH value of the reaction solution was adjusted with aqueous sodium hydroxide solution to ∼4.5. The resulting reaction mixture was allowed to stir for 1/2 h. Then, it was placed in a 23 mL Teflon-lined stainless steel reactor and heated to 160 °C for 85 h. Subsequently, the reactor was allowed to cool to room temperature. At the bottom of the vessel a crystalline material had appeared. The resulting crystalline product (0.14 g, 42%) was collected by filtration, washed with water, and air-dried. Anal. Calcd for **3**, $[Pb_3(NO_3)(C_{11}H_{13}O_9N_2)]$ (**3**) ($C_{11}H_{13}O_{12}N_3Pb_3$), M_r 1000.81): Calculated: (%) C 13.2, H 1.3 N 4.1 Found: C 13.5, H 1.2, N 4.3.

X-RAY CRYSTAL STRUCTURE DETERMINATION

X-ray quality crystals of compounds **1**, **2** and **3** were grown from aqueous solutions under hydrothermal conditions. A single crystal of **1** (0.5 × 0.3 × 0.1 mm) and **2** (0.3 × 0.6 × 0.8 mm) was mounted in air. Diffraction measurements were made on a Crystal Logic dual-goniometer diffractometer, using graphite monochromated Mo−Kα radiation (λ = 0.71073 Å). Unit cell dimensions were determined and refined by using the angular settings of 25 automatically centered reflections in the range 11 < 2θ < 23°. Throughout data collection, three standard reflections were monitored every 97 reflections, and showed less than 3% variation and no decay. Lorentz, polarization, and psi-scan absorption corrections were applied by using Crystal Logic software. On the basis of unit cell dimensions, compound **1** was identified as previously reported in the literature.[19] A single crystal of **3** (0.3 × 0.3 × 0.8 mm) was taken directly from the mother liquor and immediately cooled to −93 °C. Diffraction measurements were made on a Rigaku R-AXIS SPIDER Image Plate diffractometer using graphite monochromated Mo Kα radiation (λ = 0.71073 Å). Data collection (ω-scans) and processing (cell refinement, data reduction and empirical absorption correction) were performed using the CrystalClear program package.[20] Crystallographic details are given in Table 1.

Further experimental crystallographic details for **2**: $2\theta_{max}$ = 50°, number of reflections collected/unique/used, 3937/3784-[R(int) = 0.0464]/3784; 285 parameters refined; $(\Delta\rho)_{max}/(\Delta\rho)_{min}$ = 3.241/−2.804 e/Å^3; GOF = 1.037; R/R_w (for all data), 0.0546/0.1398. For **3**: $2\theta_{max}$ = 52; number of reflections collected/unique/used, 18687/3489[R(int) = 0.0798]/3489; 295 parameters refined; $(\Delta\rho)_{max}/(\Delta\rho)_{min}$ = 2.000/−2.786 e/Å^3; GOF = 1.128; R/R_w (for all data), 0.0316/0.0752.

Table 1. Summary of Crystal, Intensity Collection and Refinement Data for [Pb(phen)(Heida)]·4H$_2$O (2) and [Pb$_3$(NO$_3$)(Dpot)]$_n$ (3)

	2	3
formula	$C_{18}H_{25}N_3O_9Pb$	$C_{11}H_{13}N_3O_{12}Pb_3$
formula weight	634.61	1000.81
T, °K	293(2)	180(2)
wavelength, λ (Å)	0.71073	0.71073
space group	triclinic $P\bar{1}$ (no.2)	triclinic $P\bar{1}$ (no.2)
a (Å)	7.108(6)	9.0129(3)
b (Å)	9.965(7)	10.0591(4)
c (Å)	15.570(10)	10.1818(4)
α, deg	98.16(3)	85.371(1)
β, deg	94.54(3)	81.985(1)
γ, deg	95.00(3)	77.670(1)
V, (Å^3)	1082.8(14)	891.76(6)
Z	2	2
D_{calcd} (Mg m^{-3})	1.946	3.727
abs.coeff. (μ), mm^{-1}	7.845	28.322
R indices[a]	R = 0.0519[b]	R = 0.0303[b]
	R_w = 0.1361[b]	R_w = 0.0744[b]

[a] R values are based on F values, R_w values are based on F^2. $R = \sum||F_o| - |F_c||/\sum|F_o|$; $R_w = [\sum w(F_o^2 - F_c^2)^2/\sum w(F_o^2)^2]^{1/2}$. [b] [(**2**):3535, (**3**):3365, refs $I > 2\sigma(I)$]

The structures of complexes **2** and **3** were solved by direct methods using SHELXS-97,[21] and refined by full-matrix least-squares techniques on F^2 with SHELXL-97.[22] Hydrogen atoms were either located by difference maps and were refined isotropically or introduced at calculated positions as riding on bonded atoms. No H-atoms for the water solvate molecules in **2** were included in the refinement. All non-hydrogen atoms were refined anisotropically. Plots of all structures were drawn using the Diamond 3.1 crystallographic package.[23]

RESULTS AND DISCUSSION

Synthesis. The hydrothermal synthesis of compound **1** was expediently pursued through a facile reaction between $Pb(CH_3COO)_2\cdot 3H_2O$ and Heida acid in aqueous solutions. The pH, at which the reaction was developed, was ∼5. The adjustment of pH was achieved through addition of aqueous sodium hydroxide. The stoichiometric reaction leading to the formation of the title compound is shown below in reaction 1.

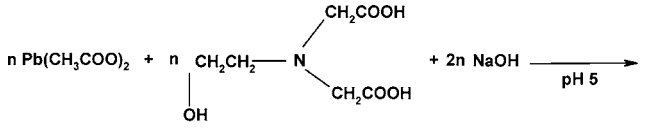

$$[Pb(C_6H_9O_5N)]_n\cdot n(H_2O)\ (1) + 2n\ CH_3COONa + n\ H_2O \quad (1)$$

In a similar reaction, $Pb(CH_3COO)_2\cdot 3H_2O$ and Heida, in a molar ratio 1:1, reacted in water with phen and aqueous sodium hydroxide at pH∼8, giving rise to compound **2**. The stoichiometric reaction leading to the formation of compound **2** is shown below in reaction 2.

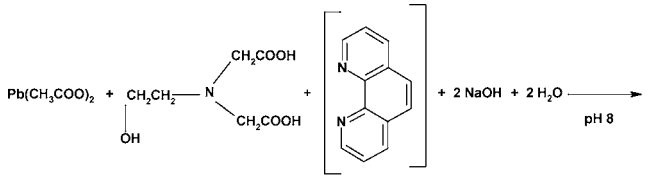

$$[Pb(phen)(C_6H_9O_5N)]\,4H_2O\ (2) + 2\ CH_3COONa \quad (2)$$

Compound **3** was the result of the reaction of $Pb(NO_3)_2$ and Dpot acid, in a molar ratio 1:1, in water at pH∼4.5 with aqueous

dx.doi.org/10.1021/ic300850g | Inorg. Chem. 2012, 51, 9282−9296

Table 2. Bond Lengths [Å] and Angles [deg] for [Pb(phen)(Heida)]·4H$_2$O (2) and [Pb$_3$(NO$_3$)(Dpot)]$_n$ (3)[a]

[Pb(phen)(Heida)]·4H$_2$O (**2**)			
Pb—O(3)	2.286(6)	Pb—N(2)	2.682(7)
Pb—O(1)	2.454(6)	Pb—N(1)	2.686(7)
Pb—N(3)	2.608(6)	Pb—O(5)	2.699(6)
O(3)−Pb—O(1)	87.4(3)	N(3)−Pb—N(1)	136.1(2)
O(3)−Pb—N(3)	69.6(2)	N(2)−Pb—N(1)	60.9(3)
O(1)−Pb—N(3)	64.8(2)	O(3)−Pb—O(5)	80.1(3)
O(3)−Pb—N(2)	90.1(2)	O(1)−Pb—O(5)	132.2(2)
O(1)−Pb—N(2)	78.6(2)	N(3)−Pb—O(5)	67.6(2)
N(3)−Pb—N(2)	138.2(2)	N(2)−Pb—O(5)	146.4(2)
O(3)−Pb—N(1)	72.0(2)	N(1)−Pb—O(5)	85.6(2)
O(1)−Pb—N(1)	133.6(2)		
[Pb$_3$(NO$_3$)(Dpot)]$_n$ (**3**)			
Pb(1)—O(5)	2.388(5)	Pb(2)—O(9)	2.556(6)
Pb(1)—O(1)	2.488(5)	Pb(2)—O(12#)	2.816(5)
Pb(1)—O(3)	2.524(6)	Pb(3)—O(4‴)	2.379(6)
Pb(1)—N(1)	2.579(6)	Pb(3)—O(2)	2.417(5)
Pb(1)—O(9′)	2.627(5)	Pb(3)—O(7‴)	2.505(6)
Pb(1)—O(8″)	2.744(6)	Pb(3)—O(11)	2.718(7)
Pb(1)—O(11)	2.851(8)	Pb(3)—O(13)	2.880(6)
Pb(2)—O(5)	2.243(5)	Pb(3)—O(1)	2.809(6)
Pb(2)—O(6)	2.419(6)	Pb(3)—O(3‴)	2.776(6)
Pb(2)—N(2)	2.493(6)		
O(5)−Pb(1)—O(1)	89.6(2)	O(4‴)−Pb(3)—O(2)	74.6(2)
O(5)− Pb(1)—O(3)	80.4(2)	O(4‴)−Pb(3)—O(7‴)	83.3(2)
O(1)− Pb(1)—O(3)	133.4(2)	O(2)−Pb(3)—O(7‴)	80.8(2)
O(5)− Pb(1)—N(1)	71.1(2)	O(4‴)−Pb(3)—O(11)	101.4(2)
O(1)− Pb(1)—N(1)	65.8(2)	O(2)−Pb(3)—O(11)	69.7(2)
O(3)− Pb(1)—N(1)	67.9(2)	O(1)−Pb(3)—O(2)	49.4(2)
O(5)− Pb(1)—O(9′)	72.4(2)	O(1)−Pb(3)—O(11)	70.3(2)
O(1)− Pb(1)—O(9′)	74.3(2)	O(1)−Pb(3)—O(13)	115.2(2)
O(3)− Pb(1)—O(9′)	141.3(2)	O(1)−Pb(3)—O(3‴)	172.3(2)
N(1)− Pb(1)—O(9′)	125.0(2)	O(1)−Pb(3)—O(4‴)	123.2(2)
O(5)− Pb(1)—O(8″)	144.5(2)	O(1)−Pb(3)—O(7‴)	80.1(2)
O(1)− Pb(1)—O(8″)	81.1(2)	O(2)−Pb(3)—O(13)	96.5(2)
O(3)− Pb(1)—O(8″)	81.4(2)	O(2)−Pb(3)—O(3‴)	124.4(2)
N(1)− Pb(1)—O(8″)	73.8(2)	O(11)−Pb(3)—O(13)	45.0(2)
O(9′)− Pb(1)—O(8″)	135.6(2)	O(11)−Pb(3)—O(3‴)	113.3(2)
O(5)−Pb(2)—O(6)	80.9(2)	O(11)−Pb(3)—O(7‴)	147.3(2)
O(5)−Pb(2)—N(2)	74.9(2)	O(13)−Pb(3)—O(3‴)	68.3(2)
O(6)−Pb(2)—N(2)	69.5(2)	O(13)−Pb(3)—O(4‴)	74.6(2)
O(5)−Pb(2)—O(9)	90.4(2)	O(13)−Pb(3)—O(7‴)	157.6(2)
O(6)−Pb(2)—O(9)	134.0(2)	O(3‴)−Pb(3)—O(4‴)	50.0(2)
N(2)−Pb(2)—O(9)	64.7(2)	O(3‴)−Pb(3)—O(7‴)	94.7(2)
O(9)−Pb(2)—O(12#)	158.5(2)	Pb(1)−O(1)—Pb(3)	144.9(2)
N(2)−Pb(2)—O(12#)	136.4(2)	Pb(1)−O(3)—Pb(3*)	152.0(2)
O(6)−Pb(2)—O(12#)	67.4(2)	Pb(2)−O(5)—Pb(1)	122.5(2)
O(5)−Pb(2)—O(12#)	92.6(2)	Pb(2)−O(9)—Pb(1′)	121.9(2)

[a]Symmetry transformations used to generate equivalent atoms: (**2**) (i) x, y, z; (ii)−x, −y, −z, **3**: (′) 1−*x*, −*y*, 2−*z*; (″) *x*, *y*, −1+*z*; (‴) *x*, −1+*y*, *z*; (*) *x*, 1+*y*, *z*; (**) *x*, *y*, 1+*z*; (#) 1−*x*, −*y*, 1−*z*.

sodium hydroxide. The stoichiometric reaction leading to the formation of compound **3** is shown below in reaction 3.

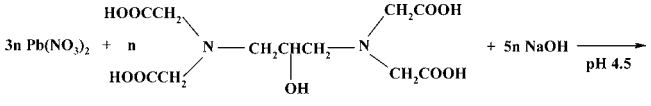

$$[Pb_3(NO_3)(C_{11}H_{13}O_9)]_n\ (3) + 5n\ NaNO_3 + 5n\ H_2O \qquad (3)$$

The derived Pb(II)-Heida and Pb(II)-Dpot materials were easily retrieved in pure crystalline form by hydrothermal synthesis. Elemental analysis of the isolated crystalline products projected the molecular formulations [Pb(Heida)]·H$_2$O (**1**), [Pb(phen)-(Heida)]·4H$_2$O (**2**), and [Pb$_3$(NO$_3$)(Dpot)] (**3**), respectively. Further spectroscopic evaluation of the crystalline products by FT-IR confirmed the presence of the ligands bound to Pb(II), thus being in line with the proposed formulations. Finally, X-ray crystallography confirmed the analytical and spectroscopic results by rendering the molecular formulation of the crystalline products in all three cases. Closely related reaction conditions leading to structurally diversified binary and

dx.doi.org/10.1021/ic300850g | Inorg. Chem. 2012, 51, 9282−9296

ternary Pb(II) species of Heida and Dpot are currently being investigated.

Compound **1** is soluble in water, in contrast to compounds **2** and **3**, which are insoluble. All three compounds are stable in the crystalline form, in the air, at room temperature for long periods of time.

Description of X-ray Structures. The structure of **1** was previously reported[19] with no synthetic details, reaction yield, quantitative analytical, and spectroscopic (FT-IR, NMR) evidence. Furthermore, no detailed presentation of the structure is either available or any relevant data exist pertaining to the lattice assembly and composition and its incipient physicochemical properties. Consequently, a detailed report on the crystal structure of **1** is presented here, with due perspective into the lattice architecture of **1** and its related ternary compound **2**.

The X-ray crystal structures of **1**, **2**, and **3** reflect molecular types of lattices. Compound **1** crystallizes in the orthorhombic space group *Pbca*, whereas compounds **2** and **3** crystallize in the triclinic space group $P\bar{1}$ (Table 1). Selected bond distances and angles for **2** and **3** are listed in Table 2. Compound **1** is a mononuclear coordination polymer (Figure 1**a**). It consists of a single Pb(II) ion and one Heida ligand bound to it. Heida is doubly deprotonated, with the sites of deprotonation being the carboxylic acid groups. Thus, binding of Heida to the Pb(II) ion leads to a zero final charge of the complex unit. The ligand is coordinated to the Pb(II) ion through the O atoms of the two carboxylate groups, the O atom of the alcohol group, and through the sp^3 N atom. The two carboxylato groups adopt different coordination modes, that is, O(1)/O(2) acts as a monodentate ligand bridging through O(1), μ_2-κ^2O, and O(3)/O(4) acts as a *syn*,*anti* bidentate bridging group. The alcohol oxygen O(5) also acts as a monodentate anchor, bridging two neighboring Pb(II) ions. Therefore, each Heida acts as a tetradentate ligand chelating around a Pb(II) ion (through O(1), O(4), O(5), and N(1)), as well as a bridging ligand to three neighboring Pb(II) ions (through O(1), O(3) and O(5)). The specific coordination of Heida promotes a layer structure for **1** which extends parallel to the crystallographic *ab* plane (Figure 1**b**), thereby forming a 2D polymer. The absence of coordination through the carboxylato oxygen O(2), which stays away from any Pb(II) and participates only in hydrogen bonding interactions to the water solvate molecule, disrupts the development of the metal–organic framework in the third direction. Conclusively, each Heida ligand binds four neighboring Pb(II) ions, and the coordination sphere of each Pb(II) ion is fulfilled by six oxygen and one nitrogen atoms belonging to four different Heida ligands, affording a coordination number 7 around Pb(II).

Considering only the bridging atoms and the metal ions, two types of rings are formed within the layered structure of **1**, that is, the 4-membered Pb(1)-O(1′)-Pb(1′)-O(5) ring and the 12-membered ring consisting of O(1′) and/or O(5) atoms, the Pb(1)-O(4)-C(3)-O(3)-Pb(1*) segment, and their symmetry related counterparts O(1*) and/or O(5**) and Pb(1**)-O(4**)-C(3**)-O(3**)-Pb(1′) correspondingly. The closest Pb···Pb interatomic distances within the above 4-membered and 12-membered rings are Pb(1)···Pb(1′) = 4.314(2) Å and Pb(1)···Pb(1*) = 6.124(2) Å. The layers are further stabilized through hydrogen bonding interactions between the alcohol group of Heida and the carboxylato oxygen O(4) of a neighboring ligand in the same layer [O(5)···O(4) = 2.562 Å (1−*x*, −*y*, −*z*), H···O(4) = 1.553 Å, O(5)−H···O(4) = 169.4 °]. Hydrogen bonds arising from the water solvate molecules link the layers together into an overall three-dimensional (3D) structure.

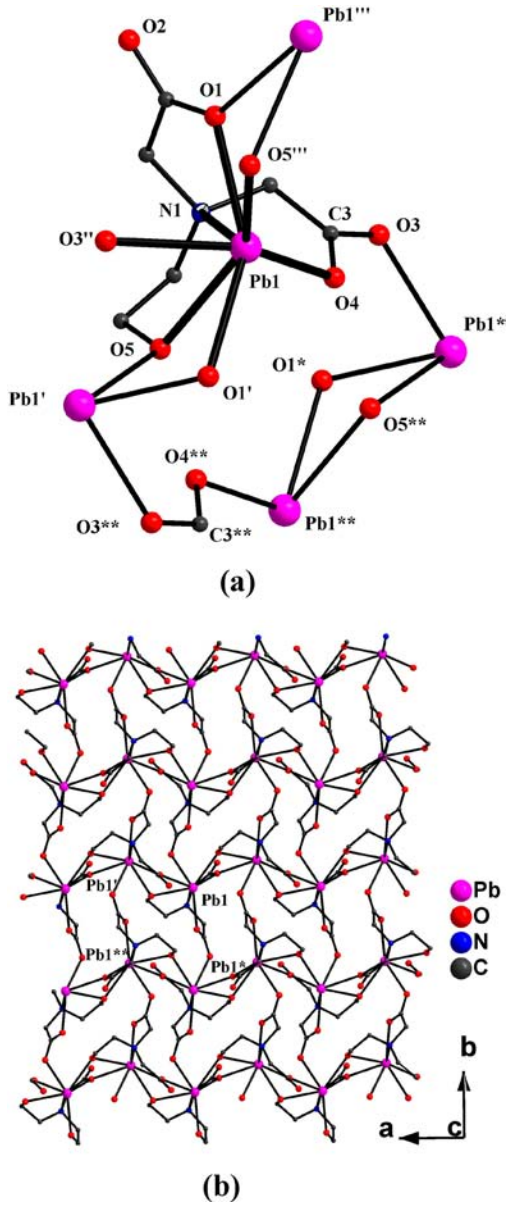

Figure 1. (**a**) Partially labeled plot of a small fragment of the structure of $[Pb(Heida)]_n \cdot nH_2O$ (**1**), showing the coordination mode of the Heida ligand. Equivalent atoms are generated by symmetry operations; (′) 0.5+*x*, 0.5−*y*, −*z*; (″) 0.5−*x*, 0.5+*y*, *z*; (‴) −0.5+*x*, 0.5−*y*, −*z*; (*) 0.5−*x*, −0.5+*y*, *z*. (**b**) A small fragment of the 2D polymer structure of **1** parallel to the *ab* plane.

Compound **2** is a ternary mononuclear assembly, consisting of a Pb(II) ion center, one Heida ligand, and one Phen molecule (Figure 2). The Pb(II) center is coordinated by one Phen molecule through its N terminals, taking up two coordination sites, and one Heida ligand coordinated through the O terminals of the carboxylate groups, the alcohol group and the sp^3 N anchor. Therefore, the Heida ligand acts as a doubly deprotonated moiety, retaining the alcohol proton and acting as a tetradentate ligand. A doubly deprotonated Heida ligand has been observed previously, coordinated with other metals such as those in $Na_2[Ni\{HOCH_2CH_2N(CH_2COO)_2\}_2]\cdot 4H_2O$,[24] $Cs_2[Co\{HOCH_2CH_2N(CH_2COO)_2\}_2]\cdot 4H_2O$,[25] $[Cu\{HOCH_2CH_2N(CH_2COO)_2\}]\cdot 2H_2O$, $\{[Mn\{HOCH_2CH_2N(CH_2COO)_2\}\cdot H_2O]\cdot H_2O\}_n$,[26] and $(NH_4)[Cr\{HOCH_2CH_2N(CH_2COO)_2\}_2]\cdot 2H_2O$.[27] In all of these compounds, the alcohol group is protonated and the two carboxylate groups

dx.doi.org/10.1021/ic300850g | *Inorg. Chem.* 2012, 51, 9282–9296

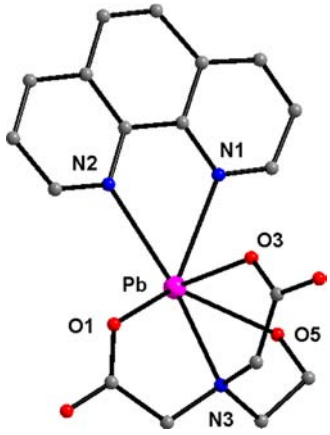

Figure 2. Partially labeled plot of the crystal structure of the $[Pb(phen)(Heida)]\cdot 4H_2O$ (**2**).

are deprotonated. Metal-Heida compounds have been reported in the literature, with the Heida ligand exhibiting variable deprotonation states and the sites of deprotonation differing from species to species. Characteristic examples include the cases of Zr(IV),[28,29] In(III),[30] V(III,IV,V),[31−34] Ni(II)[35] and Co(II).[36,37] An entirely different situation emerges in the case of the trivalent metal ions, such as Al(III), Fe(III), and Ga(III), where Heida involvement leads to multinuclear cluster assemblies and the ligand is fully deprotonated.[38−41]

On the basis of the aforementioned description, the final coordination number of Pb(II) in **2** is six. In the lattice of **2**, the neutral molecules are linked through intermolecular hydrogen bonding interactions involving the protonated alcohol group and the carboxylato oxygen atom O(4) [O5···O4 = 2.681 Å, H5O···O4 = 1.934 Å, O5−H5O···O4 = 166.0°], thus leading to polymeric hydrogen bonded chains extending parallel to the crystallographic *a*-axis. Moreover, the coordinated Phen ligands belonging to adjacent polymeric chains are parallel to each other, participating in weak $\pi-\pi$ stacking interactions, thereby resulting in the development of double chains (Figure 3**a**). Furthermore, intermolecular O···O distances in the range 2.761−2.884 Å, between the four water solvate molecules as well as the uncoordinated carboxylato oxygen atom O(2) of the Heida ligand, are attributed to intermolecular hydrogen bonding interactions, thus contributing to the stabilization of the crystal lattice and the development of a 3D framework (Figure 3**b**).

Compound **3** is a coordination polymer of Pb(II) with Dpot (Figure 4). The repeating unit in **3** consists of a trinuclear Pb(II) assembly. It contains one Dpot ligand and one NO_3^- anion, all bound to the three Pb(II) ion centers. The polymerization of this unit leads to **3**. The N terminals of the Dpot ligand (N(1) and N(2)) coordinate Pb(1) and Pb(2), respectively. The oxygen terminal O(5) from the alcohol group is coordinated to the same Pb(1) and Pb(2) centers as the N terminals, thereby acting as a bridge between the two Pb(II) centers. The O(1) terminal from the first carboxylate group is coordinated to Pb(1) and Pb(3) centers, thereby acting as a bridge, while the second carboxylate terminal O(2) from the same carboxylate group also binds the Pb(3) center. By the same token, the second carboxylate terminal O(3) acts as bridge between Pb(1) and the Pb(3*) of an abutting trinuclear assembly, while terminal O(4) coordinates to the same Pb(3*) center. In doing so, both O(1)/O(2) and O(3)/O(4) carboxylato groups act simultaneously as chelating and monodentate bridging agents between three Pb(II) ions, μ_2-κ^2O:$\kappa O'$. On the other side of the Dpot ligand, the terminal

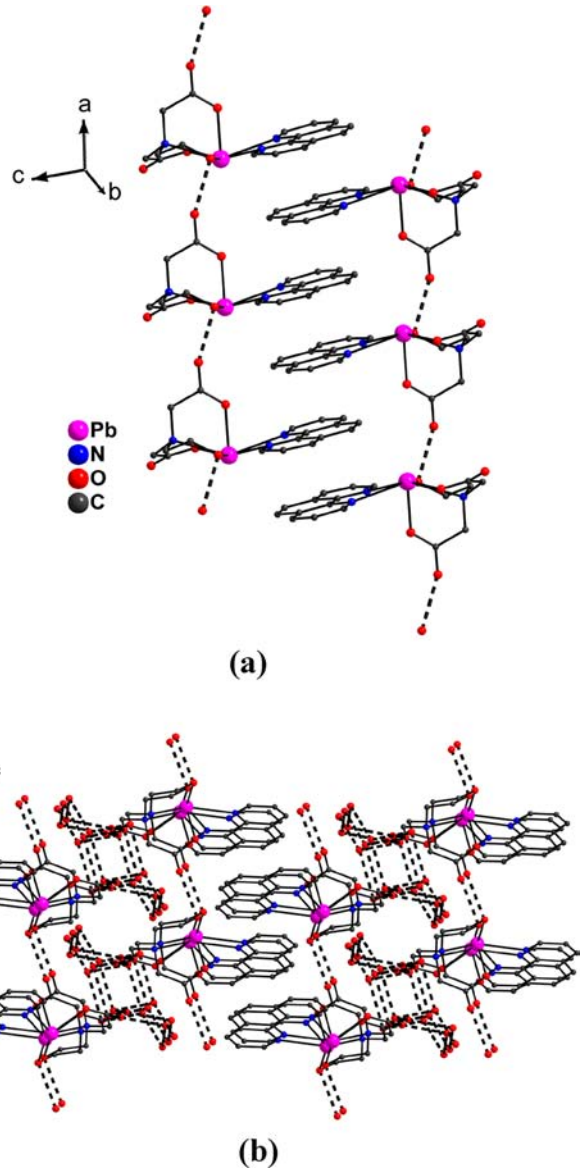

Figure 3. (**a**) Small fragment of the double chains in the lattice of **2** due to intermolecular hydrogen bonding interactions (dashed lines) and weak $\pi-\pi$ stacking interactions between the phen molecules; the double chains extend parallel to the crystallographic *a*-axis. (**b**) A small fragment of the 3D structure of **2** in the *ac* plane due to hydrogen bonding and $\pi-\pi$ interactions (see text for details).

oxygen O(6) from the third carboxylate group binds Pb(2), while carboxylate oxygen O(7) spans out to coordinate Pb(3*) previously mentioned as binding O(3) and O(4). Therefore, the O(6)/O(7) carboxylato group acts as a *syn,anti* bridging Pb(II) binder. Finally, oxygen terminal O(8) from the last carboxylate group binds to Pb(1**) from an adjacently located trinuclear Pb(II) assembly, with the O(9) terminal acting as a bridge and being coordinated to Pb(2) and Pb(1)′ from yet another abutting Pb(II) trinuclear assembly in the same lattice. In doing so, the O(8)/O(9) carboxylato group acts as a bridging agent between three Pb(II) ions, μ_3-κ^2O:$\kappa O'$. Conclusively, the four carboxylate groups of Dpot display three different coordination modes, which along with the coordination provided by the alcohol oxygen and the two nitrogen atoms, effectively bind six Pb(II) ions, namely, three Pb(1), one Pb(2), and two Pb(3) sites. Each NO_3^- anion also binds three Pb(II) ions, namely, Pb(1#),

dx.doi.org/10.1021/ic300850g | *Inorg. Chem.* 2012, 51, 9282−9296

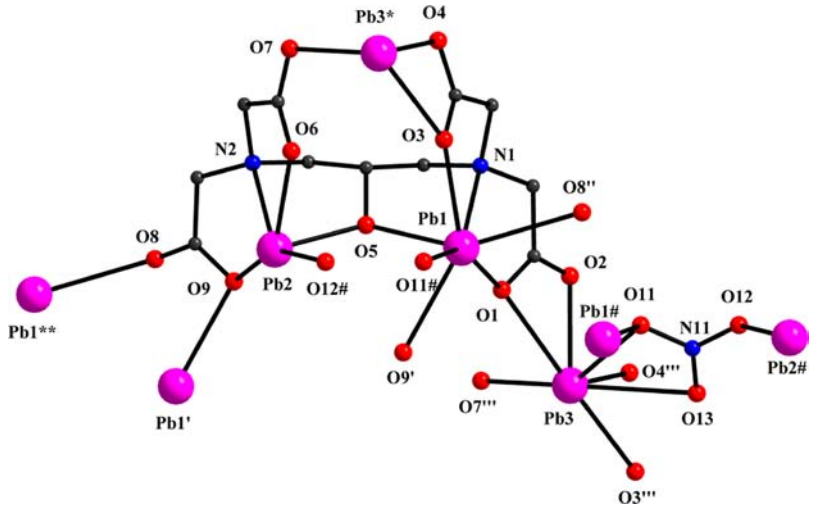

Figure 4. Partially labeled plot of a small fragment of the 2D structure in $[Pb_3(NO_3)(Dpot)]_n$ (**3**) showing the coordination mode of Dpot ligand. Equivalent atoms are generated by symmetry operations: (′) $1-x, -y, 2-z$; (″) $x, y, -1+z$; (‴) $x, -1+y, z$; (*) $x, 1+y, z$; (**) $x, y, 1+z$; (#) $1-x, -y, 1-z$.

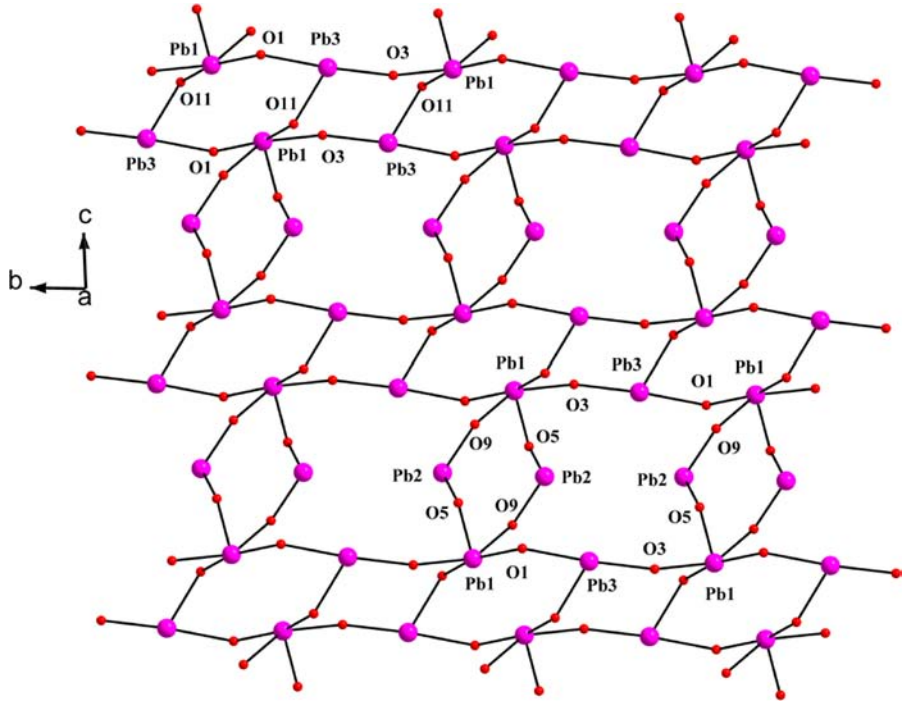

Figure 5. Partially labeled plot of a small fragment of the PbO skeleton in the structure of **3** (see text for details).

Pb(2#), and Pb(3), thus acting as a μ_3-κ^2O:$\kappa O'$:$\kappa O''$ agent. The Pb(II) ions in **3** exhibit different coordination numbers and geometries. Specifically, Pb(1) and Pb(3) display a coordination number 7, and Pb(2) has a coordination number 5.

The bridging oxygen atoms, that is, the carboxylato O(1), O(3), O(9) and the alcohol O(5) oxygen atoms of Dpot as well as O(11) of the NO_3^- anion, along with the metal ions participate in the construction of an inorganic PbO skeleton, which consists of three 8-membered and one 16-membered rings (Figure 5). Specifically, one 8-membered ring consists of the Pb(1)−O(1)−Pb(3) fragment from the same Dpot ligand and O(11) from the NO_3^- anion in one site along with their centrosymmetric counterparts. The second 8-membered ring consists of the Pb(1)−O(3)−Pb(3) fragment from the above Dpot ligand and O(11) from the above NO_3^- anion in one site along with their centrosymmetric counterparts. The third 8-membered ring consists of the Pb(1)−O(9)−Pb(2)−O(5) segment, with O(5) and O(9) belonging to the above-mentioned Dpot ligand, and their centrosymmetric counterparts. Finally, the 16-membered ring consists of the Pb(1)−O(9)−Pb(2)−O(5)−Pb(1)−O(3)−Pb(3) segment, with all oxygen atoms belonging to the same Dpot ligand, and their centrosymmetric counterparts; the two segments are linked through two O(1) anchors belonging to two different Dpot ligands. The inorganic PbO skeleton extends parallel to the crystallographic *bc* plane and is surrounded by the organic part of the Dpot ligand and the NO_3^- anion, thereby generating the overall two-dimensional (2D) structure of **3** (Figure 6**a** and 6**b**).

In all complexes, in the literature, isolated with Dpot ligand bound to metal ions, Dpot appears to be fully deprotonated, yet

dx.doi.org/10.1021/ic300850g | *Inorg. Chem.* 2012, 51, 9282−9296

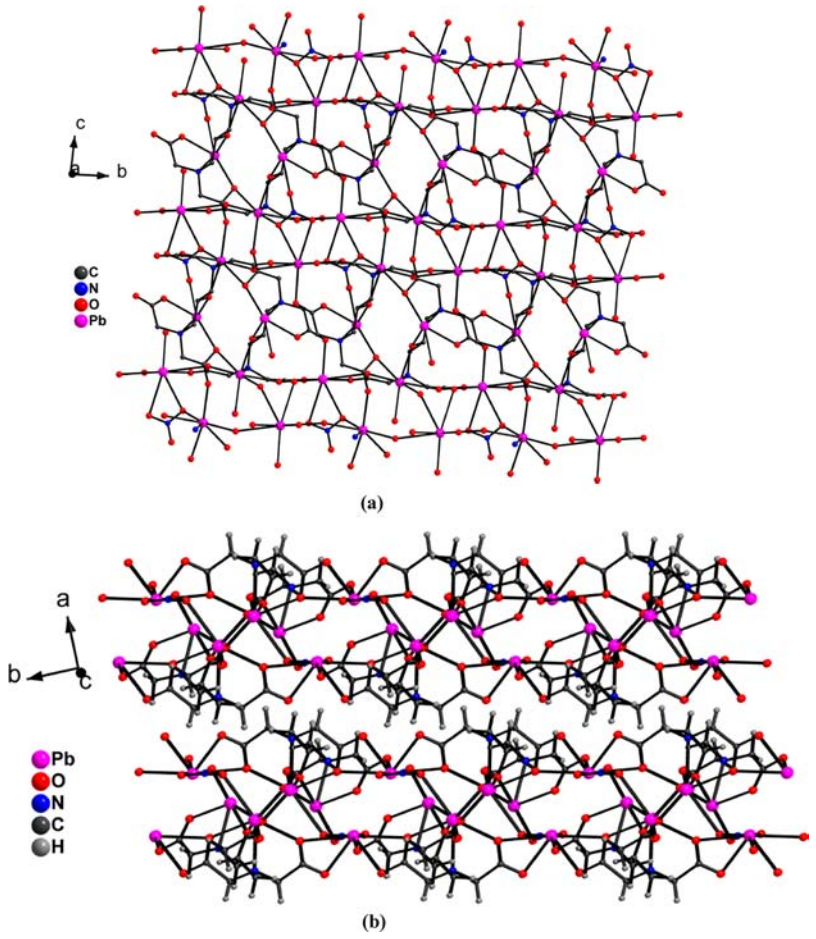

Figure 6. (a) A small fragment of the 2D structure of **3** in the *bc* plane. (b) Plot showing two adjacent layers of **3** looking down the *c*-axis.

in each case Dpot adopts a unique coordination mode upon binding metal ions. Characteristic complexes containing Dpot include $[Fe_2(Dpot)(H_2O)_3Cl]\cdot 3H_2O$,[42] $NH_4[Fe_4O(OH)(Dpot)_2(H_2O)_4]_{12}\cdot 5H_2O$,[42] $(enH_2)[Al_4(OH)_4(Dpot)_2]\cdot 7.5H_2O$,[42] $K_2[Zr_2(Dpot)_2]\cdot 5H_2O$,[43] $Na_2[Zr_2(Dpot)_2]\cdot 7H_2O\cdot C_2H_5OH$,[43] and $Cs_3[(VO)_2(O_2)_2\cdot(dpot)]$.[44]

The Pb−O bond distances in complex $[Pb(Heida)]_n\cdot nH_2O$ (**1**) are in the range 2.47(1)−3.33(1) Å,[19] in $[Pb(phen)(Heida)]\cdot 4H_2O$ (**2**) are in the range 2.286(6)−2.699(6) Å, and in $[Pb_3(NO_3)(Dpot)]_n$ (**3**) in the range 2.243(5)−2.880(6) Å. These bond distances are similar to the corresponding distances in other complexes, such as $[Pb(NNO(FA)_{0.5}]$ (2.483(8)−2.586(8) Å),[45] (NNO = Nicotinic acid N-oxide), (FA = fumaric acid), $\{[Pb_2(fum)_2(H_2O)_4]\cdot 2H_2O\}_n$ (2.517(5)−2.858(5) Å),[46] $[Pb(fum)]_n$ (2.399(5)−2.811(5) Å),[46] $[Pb(C_4H_4O_4)]$ (2.44(1)−2.91(1) Å),[47] $Pb_2(phen)_4(C_4H_4O_4)(NO_3)_2$ (2.490(3)−2.638(3) Å),[48] $[Pb(C_6H_6O_7)]_n$ (2.397(7)−2.847(1) Å),[49] $[Pb_2(C_{12}H_8N_2)_4(C_4H_2O_4)](NO_3)_2$ (2.538(3)−2.624(3) Å),[50] $[Pb_2(C_{12}H_8N_2)_4(CO_3)(C_4H_2O_4)]_n\cdot 6nH_2O$ (2.419(5)−2.868(7) Å),[50] $[Pb_2(C_{12}H_8N_2)(C_4H_2O_4)_2]_n$ (2.439(3)−2.853(3) Å),[50] and $[Pb(C_{12}H_8N_2)(C_4H_2O_4)]_n\cdot 2nH_2O$ (2.454(5)−2.768(6) Å).[50]

In $[Pb_3(NO_3)(Dpot)]_n$ (**3**), the Pb−N distances are in the range (2.493(6)−2.579(6) Å), while those in $[Pb(phen)(Heida)]\cdot 4H_2O$ (**2**) extend in the range (2.608(6)−2.686(7) Å). The Pb−N bond distances in **1**−**3** are similar to the corresponding distances in other complexes, such as $Pb_2(phen)_4(C_4H_4O_4)(NO_3)_2$ (2.508(3)−2.715(3) Å).[48]

FT-IR spectroscopy. The FT-Infrared spectra of **1**, **2**, and **3** in KBr revealed the presence of vibrationally active carboxylate groups. Antisymmetric as well as symmetric vibrations for the carboxylate groups of the coordinated ligands were present. Specifically, antisymmetric stretching vibrations $\nu_{as}(COO^-)$ for the carboxylate carbonyls appeared in the range 1593−1555 cm^{-1} for **1**, 1583−1518 cm^{-1} for **2**, and around 1573 cm^{-1} for **3**. Symmetric vibrations $\nu_s(COO^-)$ for the same groups appeared at 1397 cm^{-1} for **1**, in the range 1404−1332 cm^{-1} for **2**, and 1453−1283 cm^{-1} for **3**. The frequencies of the observed carbonyl vibrations were shifted to lower values in comparison to the corresponding vibrations in free Heida and Dpot acids, indicating changes in the vibrational status of the ligands upon binding to the Pb(II) ion. In the case of **3**, nitrate binding to the Pb(II) centers appeared in the range 1330−1380 cm^{-1}, indicating the distinct bidentate mode of coordination of the nitrate ion. Confirmation of these observations came from the X-ray crystal structure of **2** and **3**.

NMR Spectroscopy. *Solution NMR.* The solubility of **1** in water enabled us to record the solution ^{13}C NMR spectrum of **1** in D_2O (Figure 7**a**). The spectrum revealed the presence of two sets of resonances. The first set of resonances in the high field region (59.0−60.0 ppm) could be attributed to the CH_2 groups of the Heida ligand bound to the central Pb(II) ion. The second set contains a signal at 181.0 ppm in the lower field region assigned to the carbons of the carboxylate groups coordinated to the Pb(II) ion. These signals were shifted to lower fields in comparison to the resonances in pure Heida. The ^1H NMR

dx.doi.org/10.1021/ic300850g | *Inorg. Chem.* 2012, 51, 9282−9296

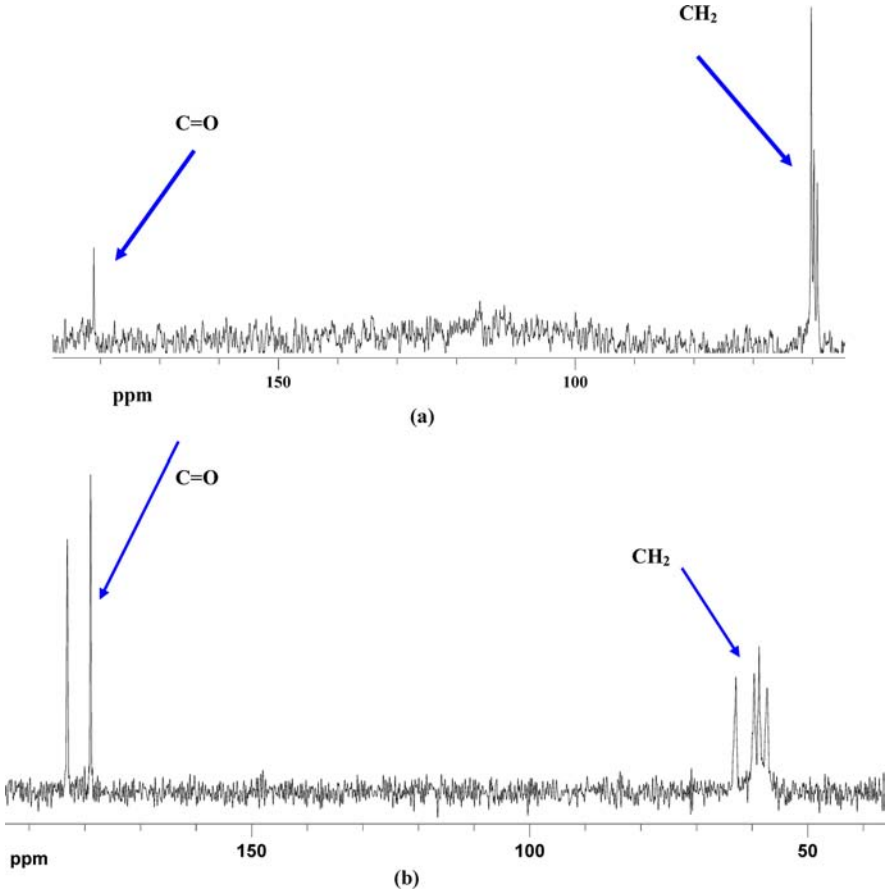

Figure 7. ^{13}C NMR spectrum of complex **1** in D_2O (**a**), and in the solid state (CP-MAS) (**b**).

spectrum of **1** in D_2O showed one resonance at 2.9 ppm and a number of resonances in the range 3.6−3.8 ppm, consistent with the presence of the methylene protons on the Heida ligand bound to Pb(II). A very small downfield shift of the proton resonances was observed compared to pure Heida.

Solid-State NMR. The Ramp CP-MAS ^{13}C NMR spectrum of **1** exhibits resonances in the high field area and two resonances in the low field area (Figure 7**b**). The group of resonances in the high field region could be attributed to the methylene carbons (54.9−62.7 ppm) located adjacent to the coordinated carboxylates and the alcohol group of the Heida ligand. Finally, in the low field region, where the carbonyl carbon resonances are expected to appear, there are two resonances at 178.8 ppm and 183.0 ppm. Both of them arise from the deprotonated carboxylated groups coordinated to Pb(II). The observed shifts were ∼5.0 ppm downfield and were comparable to that observed in the solution spectrum of **1**. It is worth noting that the pattern of resonances observed was also similar to that observed in the solution spectrum of **1**.

The spectrum of **2** exhibits a resonance in the high field region, a set of resonances in the middle, and two resonances in the low field region (Figure 8). The broad resonance in the high field area at 63.8 ppm is attributed to the methylene carbons of the Heida ligands. The resonances in the middle range 123.1−155.0 ppm are consistent with the coordination of the phen molecule in the coordination sphere of Pb(II). Finally, in the low field region, where the carbonyl carbon resonances are expected to appear, there are two resonances at 183.2 ppm and 185.5 ppm. Both of them arise from the deprotonated carboxylated groups coordinated to Pb(II).

The spectrum of **3** exhibits two resonances in the high field region and one resonance in the low field region (Figure 9), similar to the spectrum of **1**. The set of resonances in the high field region, 65.3−75.0 ppm, are due to the presence of the methylene carbons of the Dpot ligand. Finally, in the low field region, where the carbonyl carbon resonances are expected to appear, there is a set of resonances in the range 180.0−190.0 ppm for the Dpot carboxylate groups bound to the Pb(II) ion. All the resonances appear to be shifted to lower fields due to metal coordination compared to the free ligands. These observations are consistent with the structure of the compounds revealed by X-ray crystallography.

^{207}Pb-CP-MAS NMR spectra were recorded in the case of compounds **1** and **2** (efforts in the case of compound **3** did not come to fruition). The ^{207}Pb nucleus has a spin of 1/2, a fact that has been reportedly exploited to gain insight into structural features of Pb(II) compounds.[51−55] To this end, the ^{207}Pb-MAS NMR spectra of **1** and **2** were obtained. Positive chemical shift values (δ) are taken to correspond to lower shielding in comparison to the reference. The spectrum of **1** exhibits resonances in a broad range from −1100 to −2900 ppm, and the spectrum of **2** also exhibits resonances in a broad range from 100 to −2200 ppm, with the main signals bearing multiple spinning sidebands due to the large chemical shift anisotropy (Figures 10 and 11, respectively). The identity of the main resonance in each case of material (**1**, **2**) was confirmed by running experiments with variable spinning frequencies. The resonance, the chemical shift of which did not change with frequency, was the one attributed to the main resonance(s). The rest of them were side bands. On the basis of the aforementioned

dx.doi.org/10.1021/ic300850g | *Inorg. Chem.* 2012, 51, 9282−9296

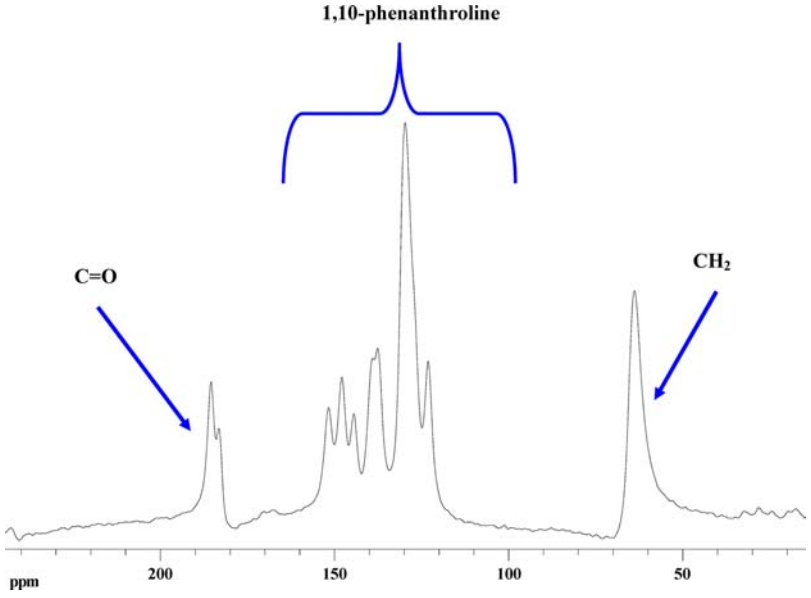

Figure 8. ^{13}C CP-MAS NMR spectrum of complex **2** in the solid state.

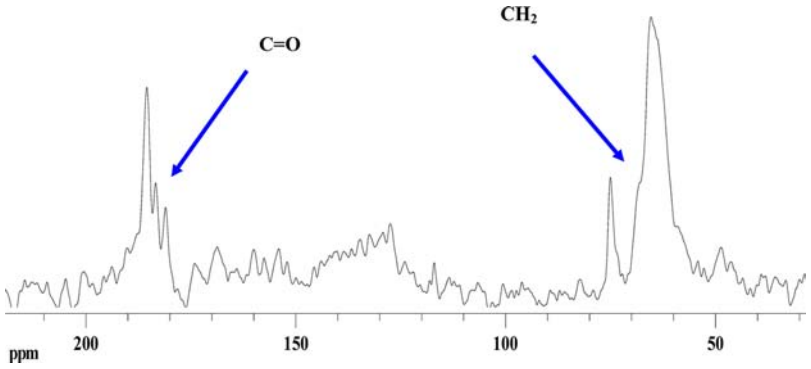

Figure 9. ^{13}C CP-MAS NMR spectrum of complex **3** in the solid state.

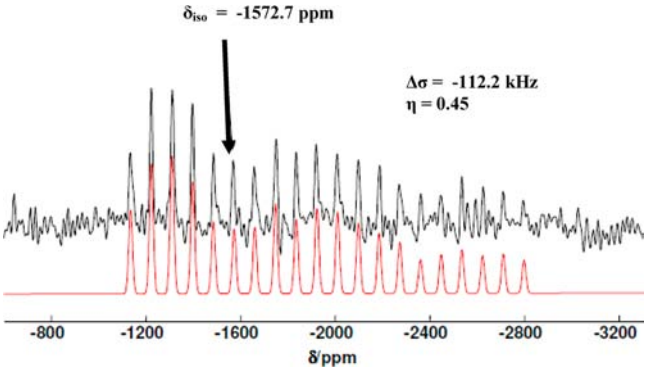

Figure 10. ^{207}Pb CP-MAS NMR spectrum of complex **1** (black) and simulated spectrum (red) in the solid state.

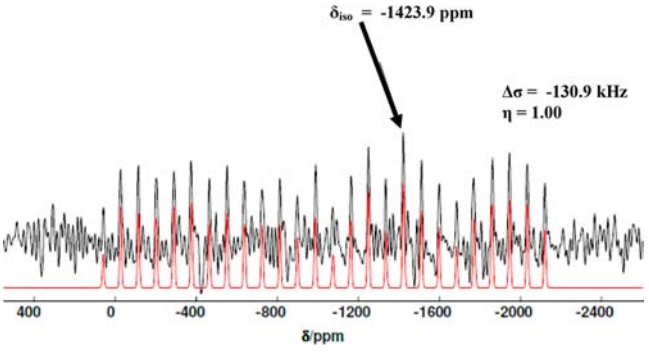

Figure 11. ^{207}Pb CP-MAS NMR spectrum of complex **2** (black) and simulated spectrum (red) in the solid state.

experiments, the spectrum of **1** exhibits an isotropic signal at −1572.7 ppm (Figure 10), whereas the spectrum of **2** exhibits an isotropic signal at −1423.9 ppm (Figure 11). The fact that only one signal each was obtained for **1** and **2** is in congruence with the crystal structure. There is no clear assignment of chemical shift ranges to metal coordination numbers, and given the fairly short difference in isotropic chemical shifts (for ^{207}Pb, shift ranges of more than 10000 ppm have been reported) still allows for assignment of the corresponding coordination number 7 and 6.

The anisotropy parameters $\Delta\sigma$ of −112.2 kHz (η = 0.45) and −130.9 kHz (η = 1.00) indicate the symmetry of the surroundings of the lead atom. These values are also quite similar and go along with the crystal structure. The ^{207}Pb chemical (isotropic and anisotropic) shifts are very sensitive to the electronic structure of Pb(II), suggesting that the coordination number and symmetry are not the only contributors to the observed chemical shifts. Further conclusions, however, would require density functional calculations of the chemical shifts, a feat which is outside the scope of the current manuscript. Unfortunately, sample **3** did not

dx.doi.org/10.1021/ic300850g | Inorg. Chem. 2012, 51, 9282−9296

yield a ^{207}Pb signal, even after three days of measurements. This could be due to an unfavorable combination of long relaxation times, low sensitivity, and large CSA values spreading the signals over a broad range. Most likely, it is probably the fact that there are three distinct Pb(II) sites present, which would disperse the signal intensity even more.

Speciation Studies. Potentiometric titrations were carried out on the ligand Heida acid alone and the binary system Pb(II)−Heida acid in various metal ion to ligand molar ratios. The neutral Heida acid exists in the "zwitterionic" form, with one of the carboxylate groups being deprotonated, having a minus one charge, while the central nitrogen is protonated. Naturally, in solution if the pH is low enough, the second carboxylate group can also be protonated, with the charge of the ligand in that case being 1+. The acidity (pK) of the carboxylic functions are quite low (pK_{a1} = ∼1.2, pK_{a2} = 2.24, with the accuracy of the determination of the first pK being limited), because of the positively charged nitrogen, and the possibility of intramolecular H-bond formation. The pK_a values were found to be very close to the values reported by Anderegg (pK_{a1} = 1.46, pK_{a2} = 2.24).[56] The nitrogen loses its proton with a pK_{a3} = 8.59. No sign of deprotonation of the alcohol−OH group was detected in the measured 2.0−11.5 pH range.

The obtained metal ion-ligand titration curves were evaluated through different potential speciation models. An acceptable fit between the experimental and the calculated titration curves for the binary Pb(II)−Heida acid system was achieved by considering the species $[PbA]^0$, $[PbAH_{-1}]^-$, and $[PbA_2]^{2-}$ (where A = Heida^{2-}, AH_{-1} = Heida^{3-}, or Heida^{2-} and OH^-) toward the end of the investigated pH range (Figure 12). The fit

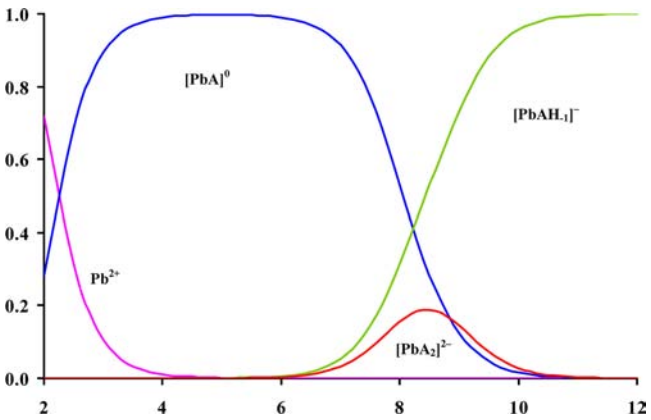

Figure 12. Speciation curves for complexes forming in the binary Pb(II)−Heida acid system; c_{Pb} = 0.001 mol dm^{-3}, c_{ligand} = 0.003 mol dm^{-3}. Charges are omitted for clarity.

was reasonably good in the overall employed pH and concentration range, indicating that the adopted speciation model had been satisfactorily defined. Other binary Pb(II):Heida complexes, including variably protonated and deprotonated species, were rejected by the computer program (PSEQUAD) during the computational process. The omission of any of the metal−ligand species decreased the fit by at least 25%. Consequently, it can be stated that the proposed speciation model, with stability constants listed in Table 3, is the best model describing the solution state of the Pb(II)−Heida binary system in the pH and concentration range studied. The uncertainties (3SD values) of the stability constants are given in parentheses. The species emerging from the speciation distribution of the

Table 3. Proton (log K) and Pb(II)−Heida Complex Formation Constants (log β) at I = 0.20 M[a]

			literature data	
species	log β ± (3SD)	pK	log β-IDA	log β-NTA
$[PbAH]^+$			10.36	13.7
$[PbA]^0$	9.20 ± 1	8.24	7.31	11.4
$[PbAH_{-1}]^-$	0.97 ± 1			
$[PbA_2H]^-$			12.7	
$[PbA_2]^{2-}$	11.98 ± 10			12.8
Fit (ml)	4.14×10^{-3}			
ref.			58[b]	59[c]

[a]Collection data at 25 °C. [b]I = 0.50 M $NaClO_4$. [c]I = 0.10 M KNO_3.

binary system are basically in line with the overall structural characteristics encountered in species **1**, which was synthesized and isolated in the solid state. The collective data indicate that the seven-coordinate octahedral geometry, observed in the solid state species **1**, does not persist in solution. On the basis of the analytical and crystallographic data, the alcohol group of the Heida retains its proton upon binding Pb(II).

As Heida acid contains N-atoms and carboxylate groups, the speciation models and stability constants can be compared with the congener ligand binary systems containing IDA and NTA.[57,58] On the basis of the significant difference between the stability of the $[PbA]^0$ complexes of Heida and IDA (Table 3), it is clear that the alcohol−OH is coordinated to Pb(II), with the Heida ligand behaving as a tetradentate ligand in solution as well as in the solid state (see **1**). However, it has been proven by pH potentiometric, NMR, and CD spectroscopic methods that Pb(II) may induce deprotonation of the weakly acidic alcohol−OH such as that in complex **3**, where the Dpot ligand is fully deprotonated. On the basis of this, we propose as an event the deprotonation of the alcohol−OH but not the departure of a water molecule from the coordination sphere, when the $[PbA]^0$ loses one proton and a species with a composition of $[PbAH_{-1}]^-$ forms. No Pb(II) ternary hydroxo species was observed either with IDA or with NTA.

What emerges as a noteworthy observation from the aqueous speciation scheme is the 1:1 Pb(III):Heida stoichiometry for the majority of the species present in it. The speciation diagram, even at 1:3 metal to ligand ratio, shows a dominance of the mononuclear 1:1 complexes $[PbA]^0$ and $[PbAH_{-1}]^-$ (Figure 12). In the early part of that range up to pH 6.5, there is only one complex $[PbA]^0$. From pH 8.5 up to pH 12.0, the predominant species is $[PbAH_{-1}]^-$. In the range pH 6.5−pH 10.0 all three species coexist. The binding mode of the Heida ligand(s) could be envisioned to proceed through the two carboxylate groups, the nitrogen and the protonated or deprotonated β-alcohol−OH as in **1** and **2**. Accordingly, it is very probable that the tetradentate coordination mode is the reason why formation of the bis-complexes is hindered. The binding mode in the bis-complex is problematic and formation of isomeric structures can not be ruled out.

DISCUSSION

Closer Look at the Aqueous Pb(II)-(O,N-Carboxylic Acid) Chemistry. In the present work, the aqueous synthetic chemistry of Pb(II) with two different, yet structurally congener, carboxylic acids was investigated under pH-specific hydrothermal conditions. Heida was employed in the study aiming at the complete structural speciation in a binary system with Pb(II), followed by an extension of the observed chemical reactivity into

dx.doi.org/10.1021/ic300850g | Inorg. Chem. 2012, 51, 9282−9296

a second ternary system encompassing Phen. The investigation of the binary system of Pb(II) with Heida led to the isolation of a coordination polymer $[Pb(Heida)]_n \cdot nH_2O$ (**1**). The arising Pb-Heida entity in **1** stands in consonance with the aqueous solution speciation studies of the specific binary system (vide infra). Concomitantly, the synthetic investigation of the ternary system of Pb(II)-Heida-Phen led to the mononuclear complex $[Pb(phen)(Heida)]\cdot 4H_2O$ (**2**), thereby disrupting the emergence of the polymeric lattice observed in **1** and affording a discrete ternary complex. Ultimately, the investigation of the binary system Pb(II)-Dpot led to the isolation of the trinuclear coordination polymer $[Pb_3(NO_3)(Dpot)]_n$ (**3**), exhibiting unique lattice features on account of the involvement of Dpot as a congener multidentate, multimodal, and bulkier substrate compared to Heida.

The structural differentiation of the lattices between **1** and **2** is a result of the presence of the Phen ligand, coordinated to Pb(II) in a bidentate fashion. Pb(II) in **1** is seven coordinate and all coordination sites are taken up by O and N atoms belonging to Heida ligands. In **2**, the Pb(II) center is six coordinate, with the coordination sites being occupied by O and N anchors of the Heida ligand and N terminals of the Phen ligand. Hence, the O and N atoms coordinated to Pb(II) in **1** originate in the same ligand, and no additional neighboring ligand interferes with the coordination around the unique Pb(II) center as seen in **2**. The Phen ligands in abutting assemblies of the crystal lattice in **2** are almost parallel to each other and participate in weak $\pi-\pi$ stacking interactions, which further contribute to the stability of the compound. It is worth mentioning that the Heida ligand is doubly deprotonated in both **1** and **2**, thereby signifying the changes observed in the coordination sphere of Pb(II) and the influence exerted in the emergence of the lattice architecture in **2**.

In the chemical reactivity of the binary system Pb(II)-Dpot leading to the ternary species $[Pb_3(NO_3)(Dpot)]_n$ (**3**), the three Pb(II) ions present themselves as unique centers formulating a trinuclear assembly as the repeating unit of the polymeric coordination compound. From coordination number 5 (Pb(2)) to coordination number 7 (Pb(1), Pb(3)), the distinct mode of Dpot binding in each case promotes diversity in the geometry and the nature of the assembled cluster.

Overall, there is a consistent fashion of developing chemical reactivity in the binary (aqueous speciation and synthetic) and ternary systems of Pb(II) with Heida/Phen and the related Dpot substrate, producing well-defined, discrete, crystalline, polymeric and nonpolymeric coordination compounds with lattice assemblies reflecting the chemical and structural nature of the two involved ligands.

Lattice Architectural Diversity in Binary and Ternary Pb(II)-(O,N) Hybrid Systems. Compound $[Pb(Heida)]_n \cdot nH_2O$ (**1**) reveals a mononuclear repeating unit 2D coordination polymer (which extends to 3D through hydrogen bonds) where one Pb(II) center is bound by one Heida ligand. Aqueous speciation studies were crucial at this juncture, suggesting the nature and salient structural features of binary species arising in solution as a function of pH and Pb(II)-Heida molecular stoichiometry. In this regard, speciation studies show that the mononuclear species [PbA] (A = $Heida^{2-}$) is the predominant species in the pH range 2−9, with no other species present in the pH range 4−6.5. To synthesize and isolate, in the solid state, new species based on the proposed binary Pb-Heida mononuclear assembly, likely exhibiting different and unique lattice architectures, attention was focused onto the ternary system of Pb-Heida-Phen. The pH-specific synthetic study of this system led to the isolation of a new compound $[Pb(phen)(Heida)]\cdot 4H_2O$ (**2**), which is no longer a coordination polymer but a monomer, further linked through intermolecular hydrogen bonding interactions to one-dimensional (1D) chains. The molecule of 1,10-phenanthroline bound to the Pb(II) center positions itself in the coordination sphere of Pb(II) in such a way that it contributes to the formation of double chains involving $\pi-\pi$ interactions in a single direction as shown in Figure 3. In this regard, the new lattice differs from that of the original coordination polymer in **1**. It is based on a mononuclear assembly and projects the importance of hydrogen bonding and $\pi-\pi$ interactions in the emergence of double chains, thereby extending the dimensionality of the lattice to 3D. Undoubtedly, the well-defined nature of **1** and **2** and the structural composition of the respective lattices, formulate the basis of synthetic interventions in the arisen lattice of **1** (and to that end of any such prototype compound) so as to induce predictable lattice changes through the involvement of a bulky ligand (i.e., Phen) dictating its structural influence in a ternary system chemical reactivity. Such approaches in the design of new variable dimensionality (1D−3D) lattices in Pb(II) binary and ternary systems are currently pursued in our laboratories. Collectively, the structural speciation approach (aqueous studies along with pH-specific hydrothermal synthesis) adopted emerges quite powerful in providing links between reactivity and solid state lattice assembly in binary and ternary Pb(II)-Heida/Phen systems (vide infra).

Poised, to this end, to pursue the synthesis of unique binary and ternary complexes of Pb(II) with multidentate ligands, dictating unique lattice architectures, we opted for a structurally congener, multidentate ligand bulkier than Heida, yet containing both carboxylate, nitrogen atom, and alcohol moieties acting as coordination anchors, that is, Dpot. The synthetic investigation of this binary system led to the isolation of a new trinuclear coordination polymer $[Pb_3(NO_3)(Dpot)]_n$ (**3**), with the repeating unit cluster (a) containing three uniquely defined Pb(II) ions from the coordination point of view, (b) involving all Pb(II) centers bound to Dpot and a NO_3^- ion, and (c) formulated so as to coordinatively promote polymerization of the basic trinuclear unit leading to the assembly of a 2D structure with a unique architecture.

Coordination Geometry of Pb(II). It has been reported that the coordination geometry of the PbO_n polyhedra in Pb(II) materials can be described as hemidirected for low coordination numbers (2−5) or holodirected for high coordination numbers (9,10), with either a hemidirected or holodirected stereochemistry being observed for intermediate coordination numbers (6−8).[59,60] It has been found through ab initio molecular orbital calculations on Pb(II) complexes in the gas-phase that a hemidirected geometry occurs if the ligands are hard, the ligand coordination number is low, and attractive interactions exist between the ligands.[61,62] To this end, the seven coordinate Pb(II) centers in **1** exhibit a hemidirected geometry. For the six coordinate Pb(II) centers in **2**, a hemidirected geometry is observed. In **3**, the seven-coordinate Pb(1) centers exhibit a holodirected geometry, the five-coordinate Pb(2) centers exhibit a hemidirected geometry, and the seven-coordinate Pb(3) centers also exhibit a hemidirected geometry. In view of the aforementioned assignments on the coordination geometry of the title complexes, the X-ray crystal structures of the investigated species concur with the analytical and physicochemical data (FT-IR and heteronuclear NMR in the solid state and in solution) on all three species. To this end, significant information emerges from the NMR of the coordination compounds in the solid state, with the ^{207}Pb signals in the CP-MAS NMR spectra

dx.doi.org/10.1021/ic300850g | Inorg. Chem. 2012, 51, 9282−9296

denoting the specific coordination geometry observed in the investigated centers of the corresponding lattice architectures. On the basis of past reports, various patterns had been observed, earmarking specific regions in the ^{207}Pb spectrum for five up to ten coordinate Pb(II) ions.[63−66] Consistent with the above information, ten coordinate Pb(II) compounds exhibit resonances as follows: $[Pb_2(HArg)_3(H_2O)(NO_3)_7]\cdot 3H_2O$ Pb1: −1285 ppm and Pb2: −2511 ppm.[64] Eight coordinate Pb(II) compounds show resonances as follows: $[Pb(OH_2)_2(Val)(Ile)(NO_3)_2]$ (from −1950 to −1790 ppm).[64] Seven coordinate Pb(II) compounds exhibit ^{207}Pb resonances as follows: $[Pb(Leu)(NO_3)]$ (−929 ppm for site 1 and −969 ppm for site 2),[63] $[Pb(HIle)_2(NO_3)(H_2O)_2](NO_3)$ (−1774 ppm),[63] $[Pb(HAsp)(NO_3)]$ (−2439 ppm),[63] $[Pb_2(HVal)_5](ClO_4)_4\cdot 2H_2O$ (from −1390 to −1755) ppm),[63] $[Pb(OH_2)(Ile)_2][NO_3]_2\cdot H_2O$ (−1766 ppm),[64] while six coordinate Pb(II) species exhibit ^{207}Pb resonances at a lower field, with a representative species being $[Pb(OH_2)_2(Val)_2(NO_3)](NO_3)$ (−1707 ppm).[64] In the present work, the arisen ^{207}Pb data are consistent with coordination numbers six (**2**) and seven (**1**), thereby earmarking the importance of that nucleus in the detection of specific lattice structural properties of Pb(II)-containing inorganic−organic hybrid materials. More work in this direction is under way in our laboratories.

Correlation between Aqueous Speciation Studies and Synthetic Assembly in the Binary Pb(II)-Heida System. The aqueous speciation in the binary Pb(II)−Heida acid system (Figure 12) can be described satisfactorily by considering the presence of Pb(II)(aq), 1:1 ($[PbA]^0$ and $[PbAH_{-1}]^-$) and 1:2 ($[PbA_2]^{2-}$) Pb(II)−Heida species. At very low pH values up to pH 4, the aquated and free of ligand coordination Pb(II) ion emerges at dwindling concentrations with increasing pH values. The predominant species in the wider pH range up to 8 was the 1:1 species dubbed [PbA]°. The stoichiometry and the zero charge on the complex are features consistent with the solid state structure of the coordination polymer and project the nature of the repeating unit, the bound water molecules of which are fully replaced by adjacently located units, thereby linking abutting mononuclear assemblies into the polymer lattice observed in **1**. Due attention to the mononuclear nature of such a repeating unit substantiates the contentions made and is satisfactorily projected into the structure of the mononuclear complex in **2**, where the bulky ternary Phen Lewis base occupies vacant coordination sites and, acting as an efficient chelator, aids in the isolation of the stable species in the solid state. In the pH range 6.5−11, a 1:2 $[PbA_2]^{2-}$ species arises. The total fraction of the 1:2 species reaches a maximum ∼20% at pH 8.5, quite lower than the 1:1 species [PbA]° present in the lower pH range overlapping that of the 1:2 species. The well-defined thermodynamic parameters in the speciation distribution attest to the presence of the 1:1 and 1:2 species as well as their position and relative concentrations in the reaction medium. The Heida ligand is a potentially tetradentate metal ion binder. Therefore, formation of a bis-complex with Pb(II) may grow less likely as the number of ligands around Pb(II) increases. To this end, coordination of a second Heida ligand to the 1:1 species, thereby intruding into the coordination sphere of Pb(II), appears to be hindered, as that is demonstrated by the low log $K(PbA_2)$ value of 2.78 and the very high $\log[K(PbA)/K(PbA_2)]$ value of 6.42. Furthermore, at higher pH values extending from 6.5 to 12, the species that gradually reaches concentrations amounting to 100% beyond pH 11 is dubbed $[PbAH_{-1}]^-$. Theoretically, this species can be a mixed hydroxo ternary complex (**1**) or as in the case of the congener Dpot ligand, a complex with the alcohol−OH losing its proton (**2**). No ternary Pb(II) hydroxo complexes, however, were detected either with IDA or NTA, a fact which clarifies that the second process likely takes place. The predominance of such species is a logical consequence of the hydrolytic chemistry of the binary Pb(II)-Heida system, revealing the potential interactions between the two reagents and their significance in dictating synthetic approaches to isolating well-defined compounds in the solid state.

On the basis of the aforementioned observations, it is logical to juxtapose the results of the aqueous speciation with the solid-state structure of compound **1** and its physicochemical properties in the solid state and in solution. To that end, the solid-state structure of **1** reveals a mononuclear Pb(II)-Heida repeating unit, with the central metal ion coordinated by four different doubly deprotonated Heida ligands, thereby filling all of the seven available coordination sites. In solution, the NMR data obtained for **1** upon dissolution and at the equilibrium state suggest that the species attains a solid-state equivalent, mononuclear, repeating unit structure. The new species likely encompasses one Pb(II) ion and one doubly deprotonated Heida ligand, with the remainder of vacant sites occupied by water molecules.

■ CONCLUSIONS

pH-Specific hydrothermal synthetic reactions of Heida and Dpot acids with Pb(II) salts afforded three new metal−organic framework compounds **1**−**3**. Compound **1** is a binary mononuclear repeating unit coordination polymer of Pb(II) with Heida, exhibiting a 2D coordination polymer extending to 3D through H-bonding interactions.[19] Compound **2** is a ternary mononuclear compound of Pb(II)-Heida-phen, with phen disrupting the binary lattice in **1** and influencing the nature of the ultimately arising ternary 3D lattice. The third compound is a 2D polymer of Pb(II)-Dpot based on trinuclear repeating units. The investigated chemical reactivity of Pb(II) at the binary and ternary level toward the two (hydroxy)carboxylic acids revealed the flexibility of Pb(II) coordinating through the O and N anchors of the related Heida and Dpot ligands, exhibiting diverse modes of coordination and promotion of distinct lattice architectures of variable dimensionality. The well-defined hydrothermal synthetic conditions were critical for the ultimate isolation of pure and well-defined crystalline products amenable to solid state and solution characterization, where possible. Compounds **1**−**3** (a) display a unique crystal lattice composition with distinct coordination number and geometry of bound ligands, (b) exhibit structural features reflecting the significance of hydrogen bonding and $\pi-\pi$ interactions in assembling 2D or 3D lattice architectures, (c) exemplify the diversity of lattice structure, composition, and properties originating in binary and ternary aqueous systems of the same metal ion (i.e., Pb(II)) reacting under specific hydrothermal conditions with increasingly multidentate and bulkier ligand-substrates, and (d) project a distinct correlation between aqueous solution reactivity chemistries with the arising crystal lattice architecture and spectroscopic signatures. Consequently, further (a) perusal targeting the rationalization of the diverse chemical reactivity observed for Pb(II) in the presence of other members of the organic (O,N)-(hydroxy)carboxylic acid family, (b) in-depth understanding the factors governing metal-linked (O,N)-(poly)-carboxylic acid promotion of variable dimensionality lattice formation through metal complexation, (c) research on rational design and construction of binary and ternary Pb(II) $\pi-\pi$ containing lattices, displaying unique supramolecular structures as well as physicochemical properties (e.g., luminescence), and

dx.doi.org/10.1021/ic300850g | Inorg. Chem. 2012, 51, 9282−9296

(d) development of new hybrid Pb(II)-(O,N) materials based on the herein presented compounds as precursors, are currently pursued by our laboratories.

■ ASSOCIATED CONTENT

Supporting Information

X-ray crystal crystallographic files, in CIF format (CCDC 871731 (2) and 871732 (3)), and detailed tables of bond distances and angles are available for **2** and **3**. This material is available free of charge via the Internet at http://pubs.acs.org.

■ AUTHOR INFORMATION

Corresponding Author

*Phone: +30-2310-996-179. Fax: +30-2310-996-196. E-mail: salif@auth.gr.

Notes

The authors declare no competing financial interest.

■ ACKNOWLEDGMENTS

This work was supported by the Greek State Scholarships Foundation "IKY", the EU−ESF and Greek national funds through the NSRF-Heracleitus II program, and the project "TÁMOP-4.2./B-09/1/KONV-2010-0005 - Creating the Center of Excellence at the University of Szeged" supported by the European Union and co-financed by the European Regional Fund.

■ REFERENCES

(1) (a) Batten, S. R.; Robson, R. *Angew. Chem., Int. Ed.* **1998**, *37*, 1460. (b) Kitagawa, S.; Kitaura, R.; Noro, S. I. *Angew. Chem., Int. Ed.* **2004**, *43*, 2334. (c) Yaghi, O. M.; O'Keeffee, M.; Ockwig, N. W.; Chae, H. K.; Eddaoudi, M.; Kim, J. *Nature* **2003**, *423*, 705. (d) Janiak, C. *Dalton Trans.* **2003**, 2781. (e) Eddaoudi, M.; Moler, D. B.; Li, H.; Chen, B.; Reineke, T. M.; O'Keeffee, M.; Yaghi, O. M. *Acc. Chem. Res.* **2000**, *34*, 319.

(2) (a) Magyar, J. S.; Weng, T. C.; Stern, C. M.; Dye, D. F.; Rous, B. W.; Payne, J. C.; Bridgewater, B. M.; Mijovilovich, A.; Parkin, G.; Zaleski, J. M.; Penner-Hahn, J. E.; Godwin, H. A. *J. Am. Chem. Soc.* **2005**, *127*, 9495. (b) Ghering, A. B.; Jenkins, L. M. M.; Schenck, B. L.; Deo, S.; Mayer, R. A.; Pikaart, M. J.; Omichinski, J. G.; Godwin, H. A. *J. Am. Chem. Soc.* **2005**, *127*, 3751. (c) Payne, J. C.; Horst, M. A.; Godwin, H. A. *J. Am. Chem. Soc.* **1999**, *121*, 6850. (d) Claudio, E. S.; Horst, M. A.; Forde, C. E.; Stern, C. L.; Zart, M. K.; Godwin, H. A. *Inorg. Chem.* **2000**, *39*, 1391. (e) Fan, S.-R.; Zhu, L.-G. *Inorg. Chem.* **2006**, *45*, 7935. (f) Fan, S.-R.; Zhu, L.-G. *Inorg. Chem.* **2007**, *46*, 6785.

(3) Schmitt, W.; Baissa, E.; Mandel, A.; Anson, C. E.; Powell, A. K. *Angew. Chem., Int. Ed.* **2001**, *40*, 3578.

(4) Schmitt, W.; Anson, C. E.; Pilawa, B.; Powell, A. K. *Z. Anorg. Allg. Chem.* **2002**, *628*, 2443.

(5) Schmitt, W.; Wernsdorfer, W.; Anson, C. E.; Powell, A. K. *Chem. Commun.* **2005**, 2098.

(6) (a) Fujita, M.; Kwon, Y. J. *J. Am. Chem. Soc.* **1994**, *116*, 1151. (b) Chui, S. S.-Y.; Lo, S. M.-F.; Charmant, J. P. H.; Orphen, A. G.; Williams, I. D. *Science* **1999**, *283*, 1148. (c) Berlinguette, C. P.; Dragulescu-Andrasi, A.; Sieber, A.; Galan-Mascaros, J. R.; Gudel, H.-U.; Achim, C.; Dunbar, K. R. *J. Am. Chem. Soc.* **2004**, *126*, 6222. (d) Palii, A. V.; Ostrovsky, S. M.; Klokishner, S. I.; Tsukerblat, B. S.; Berlinguette, C. P.; Dunbar, K. R.; Galan-Mascaros, J. R. *J. Am. Chem. Soc.* **2004**, *126*, 16860. (e) Lwamoto, M.; Furukawa, H.; Mine, Y.; Uemura, F.; Mikuriya, S. I.; Kagawa, S. *J. Chem. Soc., Chem. Commun.* **1986**, 1272.

(7) (a) Leadbeater, N. E.; Marco, M. *Chem. Rev.* **2002**, *102*, 3217. (b) Skovic, C.; Colette, B.; Euan, K.; Streib, W. E.; Folting, K.; Bollinger, J. C.; Hendrickson, D. N.; Christou, G. *J. Am. Chem. Soc.* **2002**, *124*, 3725. (c) Davis, M. E. *Nature* **2002**, *417*, 813. (d) Tsuchida, E.; Oyaizu, K. *Coord. Chem. Rev.* **2003**, *237*, 213. (e) Chifotides, H. T.; Dunbar, K. R. *Acc. Chem. Res.* **2005**, *38*, 146. (f) Tsukube, H.; Shinoda, S. *Chem. Rev.* **2002**, *102*, 2389.

(8) (a) Férey, G.; Mellot-Draznieks, C.; Serre, C.; Millange, F.; Dutour, J.; Surblé, S.; Margiolaki, I. *Science* **2005**, *309*, 2040. (b) Zhao, X.; Xiao, B.; Fletcher, A. J.; Thomas, K. M.; Bradshaw, D.; Rosseinsky, M. J. *Science* **2004**, *306*, 1012. (c) Hagrman, P. J.; Hagrman, D.; Zubieta, J. *Angew. Chem., Int. Ed.* **1999**, *38*, 2639. (d) Halder, G. J.; Kepert, C. J.; Moubaraki, B.; Murray, K. S.; Cashion, J. D. *Science* **2002**, *298*, 1762. (e) Evans, O. R.; Ngo, H. L.; Lin, W. *J. Am. Chem. Soc.* **2001**, *123*, 10395. (f) Fang, Q. R.; Zhu, G. S.; Xue, M.; Sun, J. Y.; Tian, G.; Wu, G.; Qiu, S. L. *Dalton Trans.* **2004**, 2202. (g) Fang, Q. R.; Zhu, G. S.; Xue, M.; Sun, J. Y.; Wei, Y.; Qiu, S. L.; Xu, R. R. *Angew. Chem., Int. Ed.* **2005**, *44*, 3845. (h) Yang, J.; Ma, J.-F.; Liu, Y.-Y.; Ma, J.-C.; Batten, S. R. *Cryst. Growth Des.* **2009**, *9* (4), 1894. (i) Yang, J.; Ma, J.-F.; Liu, Y.-Y.; Ma, J.-C.; Batten, S. R. *Inorg. Chem.* **2007**, *46*, 6542. (j) Yang, J.; Li, G.-D.; Cao, J.-J.; Yue, Q.; Li, G.-H.; Chen, J.-S. *Chem.—Eur. J.* **2007**, *13*, 3248.

(9) Metz, G.; Wu, X. L.; Smith, S. O. *J. Magn. Reson., Ser. A* **1994**, *110*, 219.

(10) Neue, G.; Dybowski, C.; Smith, M. L.; Hepp, M. A.; Perry, D. L. *Solid State Nucl. Magn. Reson.* **1996**, *6*, 241.

(11) Massiot, D.; Fayon, F.; Capron, M.; King, I.; Le Calvé, S.; Alonso, B.; Durand, J.-O.; Bujoli, B.; Gan, Z.; Hoatson, G. *Magn. Reson. Chem.* **2002**, *40*, 70.

(12) Haeberlen, U. In *Advances in Magnetic Resonance*, Suppl. 1; Waugh, J. S., Ed.; Academic Press: New York, 1976.

(13) Sanna, D.; Micera, G.; Buglyo, P.; Kiss, T. *J. Chem. Soc., Dalton Trans.* **1996**, 87.

(14) Dyba, M.; Jezowska-Bojczuk, M.; Kiss, E.; Kiss, T.; Kozlowski, H.; Leroux, Y.; El Manouni, D. *J. Chem. Soc., Dalton Trans.* **1996**, 1119.

(15) Gabriel, C.; Menelaou, M.; Daskalakis, M.; Lakatos, A.; Kiss, T.; Mateescu, C.; Raptis, R. G.; Zoumpoulakis, P.; Salifoglou, A. *Polyhedron* **2008**, *27*, 2911.

(16) Irving, H. M.; Miles, M. G.; Petit, L. D. *Anal. Chim. Acta* **1967**, *38*, 475.

(17) Zekány, L.; Nagypál, I. In *Computational Methods for the Determination of Stability Constants*; Leget, D., Ed.; Plenum: New York, 1985.

(18) Öhman, L. O.; Sjöberg, S. *Acta Chem. Scand.* **1982**, *36*, 47.

(19) Ilyukhin, A. B.; Poznyak, A. L.; Sergienko, V. S.; Stopolyanskaya, L. V. *Kristallografiya (Russ.) (Crystallogr. Rep.)* **1998**, *43*, 812.

(20) *CrystalClear*; Rigaku/MSC Inc.: The Woodlands, TX, 2005.

(21) Sheldrick, G. M. *SHELXS-97: Structure Solving Program*; University of Göttingen: Göttingen, Germany, 1997.

(22) Sheldrick, G. M. *SHELXL-97: Structure Refinement Program*; University of Göttingen: Göttingen, Germany, 1997.

(23) *DIAMOND − Crystal and Molecular Structure Visualization*, Ver. 3.1; Crystal Impact: Bonn, Germany.

(24) Polyakova, I. N.; Polynova, T. N.; Porai-Koshits, M. A. *Koord. Khim. (Russ.) (Coord. Chem.)* **1982**, *8*, 1268.

(25) Ananéva, N. N.; Polyakova, I. N.; Polynova, T. N.; Porai-Koshits, M. A.; Mitrofanova, N. D. *M. V. Lomonosov Moscow State University. Translated from Zh. Strukt. Khim. (Russ.)* **1975**, *16*, 481.

(26) Liu, Y. Q.; Wei, Y. G.; Liu, Q.; Zhang, S. W.; Shao, M. C. *Acta Crystallogr.* **1999**, *C55*, 534.

(27) Gabriel, C.; Raptopoulou, C. P.; Terzis, A.; Lalioti, N.; Salifoglou, A. *Inorg. Chim. Acta* **2007**, *360*, 513.

(28) Antsyshkina, A. S.; Sadikov, G. G.; Samsonova, I. N.; Davidovich, R. L.; Sergienko, V. S. *Zh. Neorg. Khim. (Russ.) (Russ. J. Inorg. Chem.)* **1999**, *44*, 598.

(29) Antsyshkina, A. S.; Shkoĺnikova, L. M.; Sadikov, G. G.; Sergienko, V. S.; Davidovich, R. L. *Zh. Neorg. Khim. (Russ.) (Russ. J. Inorg. Chem.)* **1995**, *40*, 1263.

(30) Ilyukhin, A. B.; Davidovich, R. L. *Koord. Chim. (Russ.) (Coord. Chem.)* **1994**, *20*, 590.

(31) Kanamori, K.; Ishida, K.; Fujimoto, K.; Kuwai, T.; Okamoto, K. *Bull. Chem. Soc. Jpn.* **2001**, *74*, 2377.

(32) Cansy, M.; Rehder, D. *Dalton Trans.* **2004**, 839.

(33) Hamstra, B. J.; Houseman, A. L. P.; Colpas, G. J.; Kampf, J. W.; LoBrutto, R.; Frasch, W. D.; Pecoraro, V. L. *Inorg. Chem.* **1997**, *36*, 4866.

(34) Tahir, M. M.; Keramidas, A. D.; Goldfarb, R. B.; Andersin, O. P.; Miller, M. M.; Crans, D. C. *Inorg. Chem.* **1997**, *36*, 1657.
(35) Polyakova, I. N.; Polynova, T. N.; Porai-Koshits, M. A. *Koord. Chim. (Russ.) (Coord. Chem.)* **1981**, *7*, 1894.
(36) Zasurskaya, L. A.; Polyakova, I. N.; Poznyak, A. L.; Polynova, T. N.; Sergienko, V. S. *Krystallografiya(Russ.) (Crystallogr. Rep.)* **1998**, *43*, 262.
(37) Gladkikh, O. P.; Polynova, T. N.; Porai-Koshits, M. A.; Poznyak, A. L. *Koord. Chim. (Russ.) (Coord. Chem.)* **1993**, *19*, 43.
(38) Heath, S. L.; Jordan, P. A.; Johnson, I. D.; Moore, G. R.; Powell, A. K.; Helliwell, M. *J. Inorg. Biochem.* **1995**, *59*, 785.
(39) Goodwin, J. C.; Teat, S. J.; Heath, S. L. *Angew. Chem., Int. Ed.* **2004**, *43*, 4037.
(40) Heath, S. L.; Powell, A. K. *Angew. Chem., Int. Ed. Engl.* **1992**, *31*, 191.
(41) Powell, A. K.; Heath, S. L.; Gatteschi, D.; Pardi, L.; Sessoli, R.; Spina, G.; Del Giallo, F.; Pieralli, F. *J. Am. Chem. Soc.* **1995**, *117*, 2491.
(42) Schmitt, W.; Jordan, P. A.; Henderson, R. K.; Moore, G. R.; Anson, C. E.; Powell, A. K. *Coord. Chem. Rev.* **2002**, *228*, 115.
(43) Zhong, W.; Parkinson, J. A.; Parsons, S.; Oswald, I. D. H.; Coxall, R. A.; Sadler, P. J. *Inorg. Chem.* **2004**, *43*, 3561.
(44) Kanamori, K.; Nishida, K.; Miyata, N.; Shimoyama, T.; Hata, K.; Mihara, C.; Okamoto, K.; Abe, Y.; Hayakawa, S.; Matsugo, S. *Inorg. Chem.* **2004**, *43*, 7127.
(45) Zhao, Y. H.; Su, Z. M.; Wang, Y.; Fu, Y. M.; Liu, S. D.; Li, P. *Inorg. Chem. Commun.* **2007**, *10*, 410.
(46) Zhang, K.-L.; Liang, W.; Chang, Y.; Yuan, L.-M.; Ng, S. W. *Polyhedron* **2009**, *28*, 647.
(47) Foreman, M. R. J.; Plater, M. J.; Skakle, M. S. *J. Chem. Soc., Dalton Trans.* **2001**, 1897.
(48) Soudi, A. A.; Marandi, F.; Ramazani, A.; Ahmadi, E.; Morsali, A. C. *R. Chim.* **2005**, *8*, 157.
(49) Kourgiantakis, M.; Matzapetakis, M.; Raptopoulou, C. P.; Terzis, A.; Salifoglou, A. *Inorg. Chim. Acta* **2000**, *297*, 134.
(50) Gabriel, C.; Raptopoulou, C. P.; Psycharis, V.; Terzis, A.; Zervou, M.; Mateescu, C.; Salifoglou, A. *Cryst. Growth Des.* **2011**, *11*, 382.
(51) Fallon, G. D.; Spiccia, L.; West, B. O.; Zhang, Q. *Polyhedron* **1997**, *16*, 19.
(52) Greer, B. J.; Michaelis, V. K.; Katz, M. J.; Leznoff, D. B.; Schreckenbach, G.; Kroeker, S. *Chem.—Eur. J.* **2011**, *17*, 3609.
(53) Thangadurai, P.; Ramasamy, S.; Manoharan, P. T. *Eur. Phys. J. B* **2004**, *37*, 425.
(54) Kye, Y.-S.; Connolly, S.; Herreros, B.; Harbison, G. S. *Main Group Met. Compd.* **1999**, *22*, 373.
(55) Niessen, H. G.; Van Buskirk, M.; Dybowski, C.; Corbin, D. R.; Reimer, J. A.; Bell, A. T. *J. Phys. Chem. B* **2001**, *105*, 2945.
(56) Anderegg, G. *Inorg. Chim. Acta* **1986**, *121*, 229.
(57) Napoli, A.; Cignini, P. L. *J. Inorg. Nucl. Chem.* **1976**, *38*, 2013.
(58) Anderegg, G. *Pure Appl. Chem.* **1982**, *54*, 2693.
(59) Ayyappan, S.; Diaz de Delgado, G.; Cheetham, A. K.; Firey, G.; Rao, C. N. R. *J. Chem. Soc., Dalton Trans.* **1999**, 2905.
(60) Glowiak, T.; Kozlowski, H.; Erre, L. S.; Micera, G.; Gulinati, B. *Inorg. Chim. Acta* **1992**, *202*, 43.
(61) Livny, L. S.; Glusker, J. P.; Bock, C. W. *Inorg. Chem.* **1998**, *37*, 1853.
(62) Watson, C. W.; Parker, S. C. *J. Phys. Chem. B.* **1999**, *103*, 1258.
(63) Gasque, L.; Verhoeven, M. A.; Bernès, S.; Barrios, F.; Haasnoot, J. G.; Reedijk, J. *Eur. J. Inorg. Chem.* **2008**, 4395.
(64) Saunders, C. D. L. Ph.D. Thesis, Dalhousie U., Halifax, Nova Scotia, 2009.
(65) Beckmann, P. A.; Dybowski, C. *J. Magn. Reson.* **2000**, *146*, 379.
(66) Nowotny, H.; Heger, G. *Acta Crystallogr.* **1986**, *C42*, 133.